OXFORD GENETICS

GENETICS, 2021, 218(4), iyab080
DOI: 10.1093/genetics/iyab080
Advance Access Publication Date: 25 May 2021
Neurogenetics

Presynaptic Gα$_o$ (GOA-1) signals to depress command neuron excitability and allow stretch-dependent modulation of egg laying in *Caenorhabditis elegans*

Bhavya Ravi,[1,2] Jian Zhao,[3,4] Sana I. Chaudhry,[2] Rossana Signorelli,[2] Mattingly Bartole,[1,2] Richard J. Kopchock 3rd, [2] Christian Guijarro,[2] Joshua M. Kaplan,[4] Lijun Kang,[3] and Kevin M. Collins[1,2,*]

[1]Neuroscience Program, University of Miami Miller School of Medicine, Miami, FL 33136, USA,
[2]Department of Biology, University of Miami, Coral Gables, FL 33146, USA,
[3]Department of Neuroscience, Zhejiang University School of Medicine, Hangzhou, Zhejiang, China, and
[4]Department of Molecular Biology, Massachusetts General Hospital, Boston, MA 02114, USA

*Corresponding author: Department of Biology, University of Miami, 1301 Memorial Drive, Coral Gables, FL 33146, USA. Email: kevin.collins@miami.edu

Abstract

Egg laying in the nematode worm *Caenorhabditis elegans* is a two-state behavior modulated by internal and external sensory input. We have previously shown that homeostatic feedback of embryo accumulation in the uterus regulates bursting activity of the serotonergic HSN command neurons that sustains the egg-laying active state. How sensory feedback of egg release signals to terminate the egg-laying active state is less understood. We find that Gα$_o$, a conserved Pertussis Toxin-sensitive G protein, signals within HSN to inhibit egg-laying circuit activity and prevent entry into the active state. Gα$_o$ signaling hyperpolarizes HSN, reducing HSN Ca^{2+} activity and input onto the postsynaptic vulval muscles. Loss of inhibitory Gα$_o$ signaling uncouples presynaptic HSN activity from a postsynaptic, stretch-dependent homeostat, causing precocious entry into the egg-laying active state when only a few eggs are present in the uterus. Feedback of vulval opening and egg release activates the uv1 neuroendocrine cells which release NLP-7 neuropeptides which signal to inhibit egg laying through Gα$_o$-independent mechanisms in the HSNs and Gα$_o$-dependent mechanisms in cells other than the HSNs. Thus, neuropeptide and inhibitory Gα$_o$ signaling maintain a bi-stable state of electrical excitability that dynamically controls circuit activity in response to both external and internal sensory input to drive a two-state behavior output.

Keywords: GPCR; G protein; calcium; circuit; *C. elegans*; serotonin; neuropeptide; neuron; muscle; behavior

Introduction

A major goal of neuroscience is to understand how sensory signals control neural circuit activity and changes in animal behavior. Such sensory feedback informs when a behavior should begin, how long it should continue, and when it should end. Extensive evidence has shown that neuromodulators like serotonin and neuropeptides signal through G protein coupled receptors to remodel neural circuit activity and drive behavior state transitions (Jiang *et al.* 2001; Goulding *et al.* 2008; Taghert and Nitabach 2012; Oikonomou *et al.* 2019). Yet, there is no neural circuit in any organism for which we know precisely how each signaling event contributes to sensory modulation of a behavior. Small neural circuits typically found in invertebrates combine anatomical simplicity with genetic and experimental accessibility, allowing for a complete understanding of the molecular and physiological basis for a behavioral output (Marder 2012).

The *Caenorhabditis elegans* female egg-laying behavior circuit is ideally suited to study how sensory signals modulate circuit functions that underlie decision-making. As shown in Figure 1A, the circuit is comprised of two hermaphrodite specific neurons (HSNs) that synapse onto the egg-laying vulval muscles (White *et al.* 1986; Shen *et al.* 2004; Li *et al.* 2013). During ∼2 minute active states, rhythmic HSN Ca^{2+} activity releases serotonin and neuropeptides that signal to promote the excitability of the muscles, driving ejection of ∼4–6 eggs in sequence from the uterus into the environment (Waggoner *et al.* 1998; Shyn *et al.* 2003; Zhang *et al.* 2008; Collins *et al.* 2016; Brewer *et al.* 2019). External and internal sensory inputs regulate the onset of egg laying (Horvitz *et al.* 1982; Trent 1982; Sawin 1996; Aprison and Ruvinsky 2014; Ravi *et al.* 2018a), and genetic studies have identified neuropeptides, receptors, and two antagonistic heterotrimeric G proteins that signal to regulate HSN activity, neurotransmitter release, and egg laying (Schafer 2006; Ringstad and Horvitz 2008; Koelle 2018; Banerjee *et al.* 2017; Fernandez *et al.* 2020). Gα$_q$ signals through the conserved PLCβ and Trio RhoGEF effector pathways to promote neurotransmitter release and egg laying (Brundage *et al.* 1996; Lackner *et al.* 1999; Miller *et al.* 1999; Bastiani *et al.* 2003; McMullan *et al.* 2006; Williams *et al.* 2007; McMullan and Nurrish 2011). Because phorbol ester DAG-mimetics such as PMA rescue synaptic transmission defects of Gα$_q$ signaling mutants (Lackner *et al.* 1999; Williams *et al.* 2007), DAG production and recruitment of UNC-13 and/or protein kinase C effectors are thought to mediate the Gα$_q$ dependent modulation of synaptic transmission (Yawo 1999; Wierda *et al.* 2007; Lou *et al.*

Received: January 31, 2021. **Accepted:** May 18, 2021

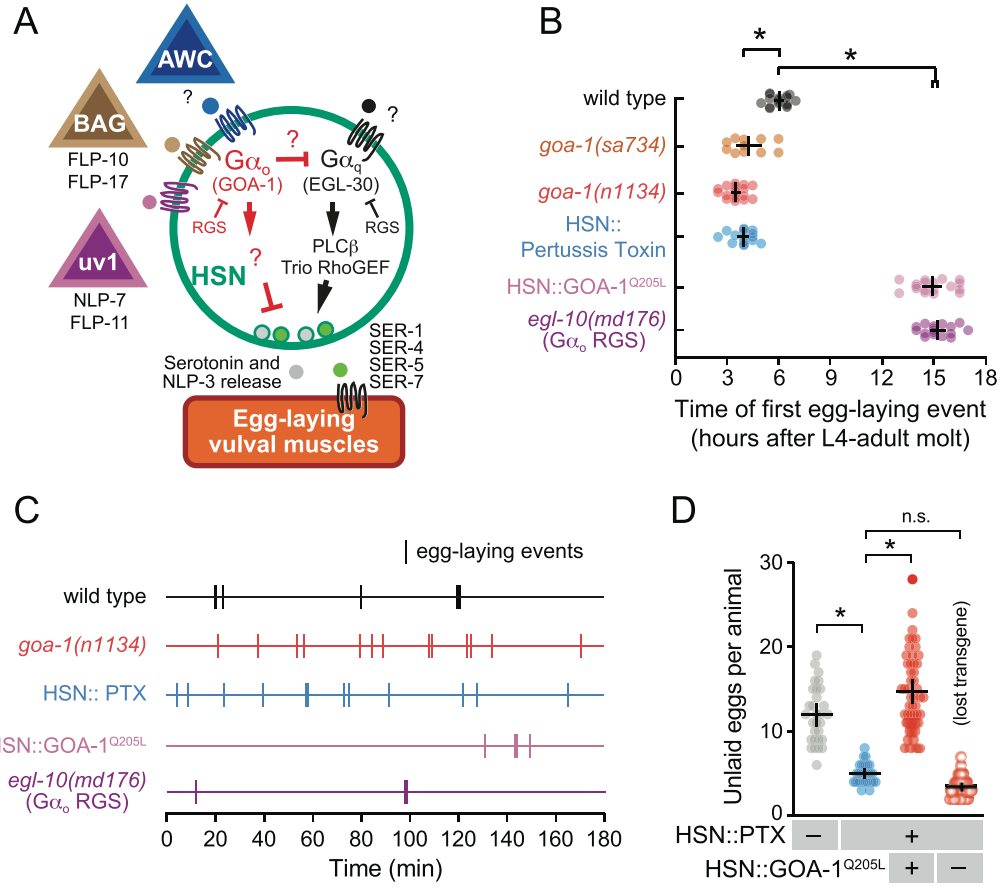

Figure 1 $G\alpha_o$ signaling maintains the inactive egg-laying behavior state. (A) Cartoon of how identified and unidentified neuropeptides released from AWC (Fenk and de Bono 2015), BAG (Ringstad and Horvitz 2008), uv1 (Banerjee *et al.* 2017), and other sensory cells bind to G-protein coupled receptors expressed on HSN command neurons (green) which signal via $G\alpha_o$ (red) or $G\alpha_q$ (black) effector pathways to modulate serotonin and NLP-3 neuropeptide release (Tanis *et al.* 2008; Brewer *et al.* 2019). The egg-laying vulval muscles (orange) express receptors for serotonin (Carnell *et al.* 2005; Dempsey *et al.* 2005; Hobson *et al.* 2006; Fernandez *et al.* 2020) and possibly NLP-3 which signal to promote vulval muscle excitability and egg laying (B) Scatter plots of the first egg-laying event in wildtype (grey), null *goa-1(sa734)* mutants (orange), hypomorphic loss-of-function *goa-1(n1134)* mutants (red), *egl-10(md176)* null mutants (purple), and transgenic animals expressing Pertussis Toxin (blue) or GOA-1^{Q205L} in the HSNs (pink). Error bars show 95% confidence intervals for the mean from ≥10 animals. Asterisks indicate $P \leq 0.0001$ (one-way ANOVA with Bonferroni correction for multiple comparisons). (C) Representative raster plots showing temporal pattern of egg laying during three hours in wild-type (black), hypomorphic loss-of-function *goa-1(n1134)* mutant (red), and *egl-10(md176)* null mutant animals (purple), along with transgenic animals expressing Pertussis Toxin (blue) or GOA-1^{Q205L} in the HSNs (pink). Vertical lines indicate single egg-laying events. (D) Scatter plots of egg accumulation in the uterus in wild-type animals (grey), transgenic animals expressing Pertussis Toxin in the HSNs (blue), transgenic animals expressing of GOA-1^{Q205L} in HSNs from the *tph-1* promoter (HSN:: GOA-1^{Q205L}, +; red), or in animals that had subsequently lost the GOA-1^{Q205L}-expressing transgenes (HSN:: GOA-1^{Q205L}, –; red open circles). Error bars indicate 95% confidence intervals for the mean. Asterisks indicate $P < 0.0001$; n.s. indicates $P = 0.2567$ (one-way ANOVA with Bonferroni's correction; $n \geq 30$ animals per genotype with five independent transgenic and nontransgenic lines analyzed).

2008). $G\alpha_q$ signaling is opposed by $G\alpha_o$ which signals to inhibit neurotransmitter release (Koelle and Horvitz 1996; Miller *et al.* 1999; Nurrish *et al.* 1999), vulval muscle activity (Shyn *et al.* 2003), and egg laying (Mendel *et al.* 1995; Segalat *et al.* 1995). How $G\alpha_o$ signaling antagonizes $G\alpha_q$, Rho, and DAG signaling is not clear. Even though $G\alpha_o$ mediates signaling by numerous neurotransmitters in diverse animals including mammals (Jiang *et al.* 2001), direct effectors for $G\alpha_o$ have not yet been identified. In *C. elegans*, $G\alpha_o$ mutants resemble animals with too much $G\alpha_q$ signaling showing increased UNC-13 localization to synapses and hyperactive egg-laying behavior defects, resembling treatment with phorbol esters (Miller *et al.* 1999; Nurrish *et al.* 1999; Jose and Koelle 2005). Because synaptic transmission could be modulated by upstream changes in cell and circuit electrical excitability and/or by downstream effects on DAG that potentiate synaptic vesicle fusion, what is needed are direct measurements of how discrete changes in G protein and effector signaling affect cell and circuit activity and their consequences on animal behavior.

Here, we explore how $G\alpha_o$ inhibits *C. elegans* egg-laying circuit activity and behavior. Our data reveal that $G\alpha_o$ signaling reduces the electrical excitability of the HSN command neurons to promote the inactive state while eggs are produced. Feedback of egg accumulation in the uterus then switches the circuit into active states where rhythmic circuit activity drives sequential egg-laying events. Thus, modulation by inhibitory $G\alpha_o$ signaling allows for proper induction of motor behavior circuit upon the alignment of optimal external and internal sensory conditions.

Materials and methods

Nematode culture and developmental staging

Caenorhabditis elegans hermaphrodites were maintained at 20°C on nematode growth medium (NGM) agar plates with *Escherichia coli* OP50 as a source of food as described (Brenner 1974). For assays involving young adults, animals were age-matched based

on the timing of completion of the L4 larval molt. All assays involving adult animals were performed using age-matched adult hermaphrodites 20–40 hours past the late L4 stage. Table 1 lists all strains used in this study and their genotypes.

Plasmid and strain construction

Calcium reporter transgenes

HSN Ca^{2+}

HSN Ca^{2+} activity was visualized using LX2004 *vsIs183* [*nlp-3::GCaMP5::nlp-3 3'UTR + nlp-3::mCherry::nlp-3 3'UTR + lin-15(+)*] *lite-1(ce314) lin-15(n765ts) X* strain expressing GCaMP5G and mCherry from the *nlp-3* promoter as previously described (Collins *et al.* 2016). To visualize HSN Ca^{2+} activity in $G\alpha_o$ signaling mutants, we crossed LX2004 *vsIs183 lite-1(ce314) lin-15(n765ts) X* males with MT2426 *goa-1(n1134) I*, DG1856 *goa-1(sa734) I*, or MT8504 *egl-10(md176) V* hermaphrodites, and the fluorescent cross-progeny were allowed to self, generating MIA210 *goa-1(n1143) I; vsIs183 X lite-1(ce314) lin-15 (n765ts) X*, MIA263 *goa-1(sa734) I; vsIs183 X lite-1(ce314) lin-15 (n765ts) X*, and MIA216 *egl-10(md176) V; vsIs183 lite-1(ce314) lin-15(n765ts) X* strains, respectively. To visualize how NLP-7 signals to inhibit HSN Ca^{2+} activity and egg laying, we crossed IZ1236 *ufIs118* hermaphrodites (Banerjee *et al.* 2017) with LX2004 males. The fluorescent cross-progeny were selfed, generating MIA293 *ufIs118; vsIs183 lite-1(ce314) lin-15(n765ts) X*. To test the requirement for $G\alpha_o$ signaling in NLP-7 inhibition, we crossed N2 males into MIA263 hermaphrodites, and the *goa-1(sa734)/+ I; vsIs183 lite-1(ce314) lin-15 (n765ts) X* heterozygous males obtained were then crossed with MIA293 hermaphrodites to generate MIA294 *ufIs118; goa-1(sa734) I; vsIs183 lite-1(ce314) lin-15(n765ts) X*. In order to test whether EGL-47 was a potential receptor for NLP-7, we crossed LX2004 males into RB850 *egl-47(ok677) V* hermaphrodites. The fluorescent cross-progeny were allowed to self and homozygous *egl-47(ok677)* mutant animals were identified by duplex PCR genotyping with the following oligos: CGTCACTTTTCCGTTGCTCTC TCATG, GTAGCGGGAAAGATGGCAAGAAGTCG, and TCGGTGA AACTCATTGTGCTCATTGTGC, creating MIA359 *egl-47(ok677) V; vsIs183 lite-1(ce314) lin-15(n765ts) X*. Wild-type N2 males were then crossed to MIA359 hermaphrodites, and the male *egl-47(ok677)/+ V; vsIs183 lite-1(ce314) lin15(n765ts) X* cross progeny were then crossed with MIA293 hermaphrodites. The cross-progeny were selfed and genotyped for the *egl-47(ok677) V* deletion mutant, generating MIA366 *ufIs118; egl-47(ok677) V; vsIs183 lite-1(ce314) lin-15(n765ts) X*.

During the course of crossing the *vsIs50* transgene expressing the catalytic subunit of Pertussis Toxin in the HSNs from the *tph-1* promoter (Tanis *et al.* 2008), we noticed linkage to the X chromosome. As such, LX850 *vsIs50 lin-15(n765ts) X* males were crossed with LX1832 *lite-1(ce314) lin-15(n765ts) X* hermaphrodites, the nonMuv progeny were selfed, and homozygous *lite-1(ce314)* nonMuv animals were kept, generating the strain MIA218 *vsIs50 lite-1(ce314) lin-15(n765ts) X*. MIA218 males were then crossed with LX2007 *vsIs186; lite-1(ce314) lin-15(n765ts) X*; the cross-progeny were selfed, generating MIA227 *vsIs186; vsIs50 lite-1(ce314) lin-15(n765ts) X*. To test whether $G\alpha_o$ acts in HSN to mediate NLP-7 inhibition, we crossed wild-type N2 males into LX2007 *vsIs186; lite-1(ce314) lin-15 (n765ts) X* hermaphrodites, and the heterozygous *vsIs186/+; lite-1(ce314) lin-15 (n765ts) X* cross-progeny were mated with IZ1236 *ufIs118* hermaphrodites. The fluorescent cross-progeny was selfed, creating MIA358 *ufIs118; vsIs186 lite-1(ce314) lin-15(n765ts) X*. Wild-type N2 males were then crossed into MIA227 hermaphrodites to generate heterozygous *vsIs186/+; vsIs50 lite-1(ce314) lin-15(n765ts) X* males which were then crossed into MIA358 hermaphrodites. The fluorescent cross-progeny were selfed, generating MIA360 *ufIs118; vsIs50; vsIs186; lite-1(ce314) lin-15(n765ts) X*. Heterozygous *vsIs186/+; vsIs50 lite-1(ce314) lin-15(n765ts) X* males were also crossed into MIA123 *egl-1(n986dm) V; lite-1(ce314) lin-15(n765ts) X* hermaphrodites, the fluorescent cross-progeny were selfed, and Egl nonMuv animals were selected, generating MIA369 *egl-1(n986dm) V; vsIs50; vsIs186 lite-1(ce314) lin-15 (n765ts) X*. The presence of the *egl-1(n986dm)* allele was confirmed with snip-SNP PCR genotyping using oligonucleotides CTCTGTTCCAGCTCAAATTTCC and GTAGTTGAGG ATCTCGCTTCGGC followed by NciI digestion.

In order to visualize HSN Ca^{2+} activity in transgenic animals expressing a constitutively active mutant GOA-1^{Q205L} protein that increases $G\alpha_o$ signaling in the HSN neurons, LX2004 *vsIs183 lite-1(ce314) lin-15(n765ts) X* males were crossed with LX849 *vsIs49; lin-15(n765ts) X* hermaphrodites. We noted linkage between the *vsIs49* transgene and the X chromosome. As such, we selected a strain MIA277 with trans-heterozygous *vsIs49* and *vsIs183* transgenes [*lite-1(ce314) vsIs49 X/lite-1(ce314) vsIs183 X*] for Ca^{2+} imaging. The MIA277 strain was maintained by picking phenotypically egg-laying defective adult animals which show GCaMP5G/mCherry expression.

Vulval Muscle Ca^{2+}

Vulval muscle Ca^{2+} activity was recorded in adult animals using LX1918 *vsIs164* [*unc-103e::GCaMP5::unc-54 3'UTR + unc-103e::mCherry::unc-54 3'UTR + lin-15(+)*] *lite-1(ce314) lin-15(n765ts) X* strain as described (Collins *et al.* 2016). To visualize vulval muscle activity in $G\alpha_o$ signaling mutants, LX1918 males were crossed with MT2426 *goa-1(n1134) I* and DG1856 *goa-1(sa734) I* hermaphrodites, and the fluorescent cross-progeny were selfed, generating MIA214 *goa-1(n1134) I; vsIs164 lite-1(ce314) lin-15(n765ts) X* and MIA295 *goa-1(sa734) I; vsIs164 lite-1(ce314) lin-15(n765ts) X* strains, respectively. To visualize vulval muscle activity in transgenic animals expressing the catalytic subunit of Pertussis Toxin in the HSN neurons (Tanis *et al.* 2008), MIA218 *vsIs50 lite-1(ce314) lin-15(n765ts) X* males were crossed with LX1919 *vsIs165* [*unc-103e::GCaMP5::unc-54 3'UTR + unc-103e::mCherry::unc-54 3'UTR + lin-15(+)*]; *lite-1(ce314) lin-15(n765ts) X* hermaphrodites, and the cross progeny were selfed, generating MIA245 *vsIs50; vsIs165; lite-1(ce314) lin-15(n765ts) X*. To visualize vulval muscle activity in transgenic animals expressing a constitutively active mutant GOA-1^{Q205L} protein which increases $G\alpha_o$ signaling in the HSN neurons (Tanis *et al.* 2008), LX849 *vsIs49; lin-15(n765ts) X* males were crossed with LX1919 *vsIs165; lite-1(ce314) lin-15(n765ts) X* hermaphrodites and the fluorescent cross-progeny were selfed, generating MIA291 *vsIs165; vsIs50 lite-1(ce314) lin-15(n765ts) X*.

Transgenes used to manipulate $G\alpha_o$ signaling and synaptic transmission in specific cells of the egg-laying circuit

HSN neurons

To test for rescue of Pertussis Toxin behavior effects through expression of GOA-1, the HSN::PTX strain (LX850) was injected with pJM70C [*tph-1::goa-1*(Q205L); 80 ng/µl (Tanis *et al.* 2008)] along with pCFJ90 [*myo-2::mCherry*; 5 ng/µl (Frokjaer-Jensen *et al.* 2008)] and pKMC42 [*tph-1::mCherry*; 80 ng/µl]. Five independent transgenic lines expressing mCherry were used for behavioral assays. Siblings that had lost the transgenic array were used as controls. One transgenic line, MIA425 [*keyEx82; vsIs50; lin-15(n765ts)*], was kept. To produce a HSN (and NSM)-specific GPB-1 expressing construct, the *gpb-1* cDNA fragment was amplified from pDEST-*gpb-1* (Yamada *et al.* 2009) using the following oligonucleotides: 5′-

Table 1 Strain names and genotypes for all animals used in this study (behavior assays and calcium imaging)

Strain	Feature	Genotype	Reference
N2	Bristol wild-type strain	Wild type	Brenner (1974)
DA521	EGL-4 (protein kinase G) gain-of-function mutant. Hyperactive egg laying, sluggish locomotion	*egl-4(ad805) IV*	Raizen *et al.* (2006)
DG1856	GOA-1 ($G\alpha_o$) null mutant, hyperactive egg laying	*goa-1(sa734) I*	Robatzek and Thomas (2000)
IZ1236	NLP-7 overexpression (*nlp-7* promoter)	*ufIs118*	Banerjee *et al.* (2017)
KG421	GSA-1 ($G\alpha_s$) gain-of-function mutant. Hyperactive locomotion	*gsa-1(ce81) I*	Schade *et al.* (2005)
KG518	ACY-1 (Adenylate Cyclase) gain-of-function mutant. Hyperactive locomotion	*acy-1(ce2) III*	Schade *et al.* (2005)
KG532	KIN-2 (protein kinase A inhibitory regulatory subunit) loss-of-function mutant. Hypersensitive to stimuli	*kin-2(ce179) X*	Schade *et al.* (2005)
KG744	PDE-4 (phosphodiesterase) loss-of-function mutant, Hyperactive locomotion	*pde-4(ce268) II*	Charlie *et al.* (2006a)
LX75	*egl-10(md176)* mutant strain for transgene production, multi-vulva at 20 °C in the absence of *lin-15(+)* rescue transgene	*egl-10(md176) V; lin-15(n765ts) X*	Patikoglou and Koelle (2002)
LX755	HSN and NSM expressing GFP + EGL-10 (*tph-1* promoter) in *egl-10* mutant background. Less egg-laying defective than LX764	*egl-10(md176) V; lin-15(n765ts) X vsEx437*	This study
LX764	HSN and NSM expressing GFP only (*tph-1* promoter) in *egl-10* mutant background. Egg-laying defective	*egl-10(md176) V; lin-15(n765ts) X vsEx439*	This study
LX849	HSN and NSM activated GOA-1(Q205L), *tph-1* promoter, egg laying defective	*vsIs49; lin-15(n765ts) X*	Tanis *et al.* (2008)
LX850	HSN and NSM Pertussis Toxin, *tph-1* promoter, hyperactive egg laying	*vsIs50; lin-15(n765ts) X*	Tanis *et al.* (2008)
LX1832	Strain for transgene production, blue-light insensitive, multi-vulva at 20°C in the absence of *lin-15(+)* rescue transgene.	*lite-1(ce314) lin-15(n765ts) X*	Gurel *et al.* (2012)
LX1918	Vulval muscle GCaMP5, mCherry (*unc-103e* promoter, *unc-54* 3' UTR)	*vsIs164 lite-1(ce314) lin-15(n765ts) X*	Collins *et al.* (2016)
LX1919	Vulval muscle GCaMP5, mCherry (*unc-103e* promoter, *unc-54* 3' UTR)	*vsIs165; lite-1(ce314) lin-15(n765ts) X*	Collins *et al.* (2016)
LX2004	HSN GCaMP5, mCherry (*nlp-3* promoter, *nlp-3* 3'UTR)	*vsIs183 lite-1(ce314) lin-15(n765ts) X*	Collins *et al.* (2016)
LX2007	HSN GCaMP5, mCherry (*nlp-3* promoter, *nlp-3* 3'UTR)	*vsIs186 lite-1(ce314) lin-15(n765ts) X*	Collins *et al.* (2016)
MIA26	No HSNs	*egl-1(n986dm) V*	Garcia and Collins (2019)
MIA36	EGL-4 (protein kinase G) gain-of-function mutant. Hyperactive egg laying, sluggish locomotion	*egl-4(mg410) IV*	Hao *et al.* (2011)
MIA123	No HSNs in *lite-1*, *lin-15* background for crossing with transgenes	*egl-1(n986dm) V; lite-1(ce314) lin-15(n765ts) X*	This study
MIA144	VC Tetanus Toxin (minimal *lin-11* promoter enhancer, *unc-54* 3'UTR)	*keyIs33; lite-1(ce314) lin-15(n765ts) X*	Kopchock *et al.* (2021)
MIA210	GOA-1 ($G\alpha_o$) reduced-function mutant; HSN GCaMP, mCherry	*goa-1(n1134) I; vsIs183 lite-1(ce314) lin-15(n765ts) X*	This study
MIA214	GOA-1 ($G\alpha_o$) reduced-function mutant; vulval muscle GCaMP5, mCherry	*goa-1(n1134) I; vsIs164 lite-1(ce314) lin-15(n765ts) X*	This study
MIA216	Increased $G\alpha_o$ signaling; HSN GCaMP5, mCherry	*egl-10(md176) V; vsIs183 lite-1(ce314) lin-15(n765ts) X*	This study
MIA218	HSN and NSM Pertussis Toxin in blue-light insensitive, *lin-15* multi-vulva background	*vsIs50 lite-1(ce314) lin-15(n765ts) X*	This study
MIA227	HSN and NSM Pertussis Toxin (*tph-1* promoter); HSN GCaMP5, mCherry (*nlp-3* promoter)	*vsIs186; vsIs50 lite-1(ce314) lin-15(n765ts) X*	This study
MIA245	HSN and NSM Pertussis Toxin (*tph-1* promoter); vulval muscle GCaMP5, mCherry (*unc-103e* promoter)	*vsIs50 X vsIs165; lite-1(ce314) lin-15(n765ts) X*	This study
MIA256	Vulval muscle mCherry (*ceh-24* promoter, *unc-54* 3'UTR)	*keyEx45; lite-1(ce314) lin-15(n765ts) X*	This study
MIA257	Vulval muscle mCherry + Pertussis Toxin (*ceh-24* promoter, *unc-54* 3'UTR)	*keyEx46; lite-1(ce314) lin-15(n765ts) X*	This study
MIA258	Vulval muscle mCherry + Activated GOA-1(Q205L) (*ceh-24* promoter, *unc-54* 3'UTR)	*keyEx47; lite-1(ce314) lin-15(n765ts) X*	This study
MIA259	uv1 cells mCherry (*tdc-1* promoter, *ocr-2* 3' UTR)	*keyEx48; lite-1(ce314) lin-15(n765ts) X*	This study
MIA260	uv1 cells mCherry + Pertussis Toxin (*tdc-1* promoter, *ocr-2* 3' UTR)	*keyEx49; lite-1(ce314) lin-15(n765ts) X*	This study
MIA261	uv1 cells mCherry + Activated GOA-1(Q205L) (*tdc-1* promoter, *ocr-2* 3' UTR)	*keyEx50; lite-1(ce314) lin-15(n765ts) X*	This study
MIA262			This study

(continued)

Table 1. (continued)

Strain	Feature	Genotype	Reference
	Vulval muscle mCherry + Tetanus toxin (*ceh-24* promoter, *unc-54* 3'UTR)	*keyEx51; lite-1(ce314) lin-15(n765ts) X*	
MIA263	GOA-1 ($G\alpha_o$) null mutant; HSN GCaMP5, mCherry	*goa-1(sa734) I; vsIs183 lite-1(ce314) lin-15(n765ts) X*	This study
MIA277	Increased $G\alpha_o$ signaling in HSN; HSN GCaMP5, mCherry	*vsIs49/+, +/vsIs183 lite-1(ce314) lin-15(n765ts) X (trans-heterozygote)*	This study
MIA278	HSN/NSM *gpb-1* and *gpc-2* overexpression + GFP (*tph-1* promoter)	*keyEx52; lite-1(ce314) lin-15(n765ts) X*	This study
MIA279	HSN/NSM empty + GFP (*tph-1* promoter)	*keyEx53; lite-1(ce314) lin-15(n765ts) X*	This study
MIA282	PDE-2 (phosphodiesterase) loss-of-function mutant	*pde-2(qj6)*	Fujiwara *et al.* (2015)
MIA291	Increased $G\alpha_o$ signaling in HSN (*tph-1* promoter); vulval muscle GCaMP5, mCherry (*unc-103e* promoter)	*vsIs49; vsIs165 lite-1(ce314) lin-15(n765ts) X*	This study
MIA293	NLP-7 overexpression (*nlp-7* promoter); HSN GCaMP5, mCherry (*nlp-3* promoter)	*ufIs118; vsIs183 lite-1(ce314) lin-15(n765ts) X*	Banerjee *et al.* (2017) and This study
MIA294	NLP-7 overexpression (*nlp-7* promoter); *goa-1*($G\alpha_o$) null mutant; HSN GCaMP5, mCherry (*nlp-3* promoter)	*ufIs118; goa-1(sa734) I; vsIs183 lite-1(ce314) lin-15(n765ts) X*	Banerjee *et al.* (2017) and This stud
MIA295	GOA-1 ($G\alpha_o$) mutant, vulval muscle GCaMP5, mCherry (*unc-103e* promoter)	*goa-1(sa734) I; vsIs164 lite-1(ce314) lin-15(n765ts) X*	This study
MIA331	GOA-1 ($G\alpha_o$) null mutant; EGL-4 (protein kinase G) null mutant	*goa-1(sa734) I; egl-4(n479) IV*	This study
MIA345	GOA-1 ($G\alpha_o$) null mutant; no HSNs	*goa-1(sa734) I; egl-1(n986dm) V*	This study
MIA359	EGL-47 null mutant; HSN GCaMP5, mCherry (*nlp-3* promoter)	*egl-47(ok677) V; vsIs183 lite-1(ce314) lin-15(n765ts) X*	This study
MIA360	NLP-7 overexpression (*nlp-7* promoter); HSN and NSM Pertussis Toxin (*tph-1* promoter); HSN GCaMP5, mCherry (*nlp-3* promoter)	*ufIs118; vsIs50; vsIs186 lite-1(ce314) lin-15(n765ts) X*	This study
MIA366	NLP-7 overexpression [*nlp-7* promoter; EGL-47 null mutant; HSN GCaMP5, mCherry (*nlp-3* promoter)]	*ufIs118; egl-47(ok677) V; vsIs183 lite-1(ce314) lin-15(n765ts) X*	This study
MIA369	No HSNs; HSN and NSM Pertussis Toxin (*tph-1* promoter); HSN GCaMP5, mCherry (*nlp-3* promoter)	*egl-1(n986dm) V; vsIs50; vsIs186 lite-1(ce314) lin-15 (n765ts) X*	This study
MIA370	VC Tetanus Toxin (*lin-11* enhancer/promoter); HSN and NSM Pertussis Toxin (*tph-1* promoter); HSN GCaMP5, mCherry (*nlp-3* promoter)	*keyIs33; vsIs186; vsIs50 keyIs33; lite-1(ce314) lin-15(n765ts) X*	This study
MIA371	GOA-1 ($G\alpha_o$) null mutant; VC Tetanus Toxin (*lin-11* enhancer/promoter)	*goa-1(sa734) I; keyIs33; lite-1(ce314) lin-15(n765ts) X*	This study
MIA425	HSN Pertussis Toxin rescued with HSN GOA-1^{Q205L} (*tph-1* promoter)	*keyEx82; vsIs50; lin-15(n765ts)*	This study
MT1073	EGL-4 (protein kinase G) loss-of-function mutant. Egg-laying defective, roaming locomotion	*egl-4(n478) IV*	L'Etoile *et al.* (2002)
MT1074	EGL-4 (protein kinase G) null mutant. Egg-laying defective, roaming locomotion	*egl-4(n479) IV*	L'Etoile *et al.* (2002)
MT2426	GOA-1 ($G\alpha_o$) reduced-function mutant, hyperactive egg laying	*goa-1(n1134) I*	Segalat *et al.* (1995)
MT8504	Increased $G\alpha_o$ signaling due to mutation in RGS protein, EGL-10	*egl-10(md176) V*	Koelle and Horvitz (1996)
RB850	EGL-47 null mutant	*egl-47(ok677) V*	Moresco and Koelle (2004) and *C. elegans* Deletion Mutant Consortium (2012)

GAGGCTAGCGTAGAAAAAATGAGCGAACTTGACCAACTTCGA-3′ and 5′-GCGGGTACCTCATTAATTCCAGATCTTGAGGAACGAG-3′. The ~1 kb DNA fragment was digested with NheI/KpnI and ligated into pJT40A (Tanis *et al.* 2008) to generate pBR30. To produce an HSN (and NSM)-specific GPC-2 expressing construct, the *gpc-2* cDNA fragment was amplified from worm genomic DNA using the following forward and reverse oligonucleotides: 5′-GAGGCTAGCGTAGAAAAAATGGATAAATCTGACATGCAACGA-3′ and 5′-GCGGGTACCTTAGAGCATGCTGCACTTGCT-3′. The ~250 bp DNA fragment was digested with NheI/KpnI and ligated into pJT40A to generate pBR31. To co-overexpress the βγ G protein subunits in the HSN neurons, we injected pBR30 (50 ng/μl), pBR31 (50 ng/μl), and pJM60 [*ptph-1*::GFP] (80 ng/μl) (Moresco and Koelle 2004) into the LX1832 *lite-1(ce314) lin-15(n765ts)* animals along with pLI5EK (50 ng/μl), generating five independent extrachromosomal transgenic lines which were used for behavioral assays. One representative transgenic strain, MIA278 [*keyEx52; lite-1(ce314) lin-15(n765ts)*], was kept. To generate a control strain for comparison in the egg-laying assays, we injected pJM66 [*ptph-1*::empty] (100 ng/μl) (Tanis *et al.* 2008) and pJM60 (80 ng/μl) into the LX1832 *lite-1(ce314) lin-15(n765ts)* animals along with pLI5EK (50 ng/μl) generating five independent extrachromosomal control transgenes which were used for behavioral assays. One representative transgenic strain, MIA279 [*keyEx53; lite-1(ce314) lin-15(n765ts)*], was kept. Strains expressing either GFP along with EGL-10 or GFP alone in the HSNs from the *tph-1* promoter were a

generous gift of Jessica Tanis and Michael Koelle. Briefly, plasmids pJT35A (100 ng/µl) expressing *egl-10* coding sequences from a cDNA and pJM60A (70 ng/µl) expressing GFP coding sequences, both from the long (3.1 kb) *tph-1* promoter, along with pL15EK (50 ng/µl) were injected into the LX75 *egl-10(md176) V; lin-15(n765ts) X* mutant strain to generate LX755 *egl-10(md176) V; lin-15(n765ts) X vsEx437* [*tph-1p::GFP, tph-1p::egl-10*]. Control animals were generated by injecting LX75 with pJM66 (100 ng/µl) expressing nothing and pJM60A (70 ng/µl) expressing coding sequences for GFP, both from the long (3.1 kb) *tph-1* promoter, along with pL15EK (50 ng/µl), generating LX764 *egl-10(md176) V; lin-15(n765ts) X vsEx439 [tph-1p::empty, tph-1p::GFP]*. To test how loss of HSNs affected the hyperactive egg-laying behavior of *goa-1(sa734)* null mutants, we mated wild-type N2 males into MIA26 *egl-1(n986dm) V* hermaphrodites, and the heterozygous *egl-1(n986dm)/+* male cross-progeny were then crossed into DG1856 *goa-1(sa734) I* hermaphrodites. Their cross-progeny were selfed, and the presence of the *egl-1(n986dm)* and *goa-1(sa734)* were confirmed by genotyping, creating MIA345 *goa-1(sa734) I; egl-1(n986dm) V*.

Vulval muscles

pJT40A *Ptph-1*::Pertussis Toxin (Tanis *et al.* 2008) was digested with NheI/KpnI and ligated into pBR3 (*Pceh-24*::mCherry) to generate pBR20. pBR20 [*Pceh-24*::Pertussis Toxin] (10 ng/µl) and pBR3 [*Pceh-24*::mCherry] (10 ng/µl) were injected into the LX1832 *lite-1(ce314) lin-15(n765ts)* animals along with pLI5EK (50 ng/µl) to generate five independent extrachromosomal transgenes which were used for behavioral assays. One representative transgenic strain, MIA257 [*keyEx46*; *lite-1(ce314) lin-15(n765ts)*], was kept. To produce vulval muscle-specific GOA-1(Q205L), the coding sequence of GOA-1(Q205L) was recovered from pJM70C (Tanis *et al.* 2008) after digestion with NheI/SacI and ligated into pKMC188 [*Punc-103e*::GFP; (Collins and Koelle 2013)] generating pKMC268 [*Punc-103e::goa-1(Q205L)*]. However, because the *unc-103e* promoter also directs expression in neurons that might indirectly regulate egg laying, GOA-1(Q205L) coding sequences were removed from pKMC268 by digesting with NheI/NcoI and ligated into pBR3 to generate pBR21. pBR21 [*Pceh-24*::GOA-1^{Q205L}] (10 ng/µl) and pBR3 [*Pceh-24*::mCherry] (10 ng/µl) were injected into the LX1832 *lite-1(ce314) lin-15(n765ts) X* animals along with pLI5EK (50 ng/µl) to generate five independent extrachromosomal transgenes which were used for behavior assays. One representative transgenic strain, MIA258 [*keyEx47*; *lite-1(ce314) lin-15(n765ts)*], was kept. To generate control strains for comparison in egg-laying assays, pBR3 [*Pceh-24*::mCherry] (20 ng/µl) was injected into the LX1832 *lite-1(ce314) lin-15(n765ts) X* animals along with pLI5EK (50 ng/µl) to generate five independent extrachromosomal transgenes which were used for behavioral assays. One representative control transgenic strain, MIA256 [*keyEx45*; *lite-1(ce314) lin-15(n765ts)*], was kept. To produce a vulval muscle-specific Tetanus Toxin transgene, Tetanus Toxin coding sequences were amplified from pAJ49 (*Pocr-2*::Tetanus toxin) (Jose *et al.* 2007) using the following oligonucleotides: 5′-GAGGCTAGCGTAGAAAAA ATGCCGATCACCATCAACAACTTC-3′ and 5′-GCGCAGGCGGCC GCTCAAGCGGTACGGTTGTACAGGTT-3′. The DNA fragment was digested with NheI/NotI and ligated into pBR6 to generate pBR27. To block any possible neurotransmitter release from the vulval muscles, pBR27 (10 ng/µl) and pBR3 (10 ng/µl) was injected into the LX1832 *lite-1(ce314) lin-15(n765ts)* animals along with pLI5EK (50 ng/µl) to generate five independent extrachromosomal transgenes which were used for behavior assays. One representative transgenic strain, MIA262 [*keyEx51*; *lite-1(ce314) lin-15(n765ts)*], was kept.

uv1 neuroendocrine cells

To generate a uv1 cell-specific Pertussis Toxin transgene, pBR20 (*Pceh-24*::Pertussis Toxin) was digested with NheI/NcoI and the coding sequences of Pertussis Toxin were then ligated into pAB5 (*Ptdc-1*::mCherry::*ocr-2* 3′UTR) to generate pBR25. pBR25 [*Ptdc-1*::Pertussis Toxin] (10 ng/µl) and pAB5 [*Ptdc-1*::mCherry] (5 ng/µl) were injected into LX1832 *lite-1(ce314) lin-15(n765ts)* animals along with pLI5EK (50 ng/µl) to generate five independent extrachromosomal transgenes which were used for behavioral assays. One representative transgenic strain, MIA260 [*keyEx49*; *lite-1(ce314) lin-15(n765ts)*], was kept. To generate a uv1 cell-specific GOA-1(Q205L) transgene, pKMC268 [*Punc-103e*::GOA-1(Q205L)] was digested with NheI/NcoI and the coding sequences of GOA-1(Q205L) were then ligated into pBR25 to generate pBR26. To increase $G\alpha_o$ signaling in uv1 cells, we injected pBR26 [*Ptdc-1*::GOA-1^{Q205L}] (10 ng/µl) and pAB5 [*Ptdc-1*::mCherry] (5 ng/µl) into the LX1832 *lite-1(ce314) lin-15(n765ts)* animals along with pLI5EK (50 ng/µl) to generate five independent extrachromosomal transgenes which were used for behavioral assays. One transgenic strain MIA261 [*keyEx50*; *lite-1(ce314) lin-15(n765ts)*] was kept. To generate a control strain for comparison in our egg-laying assays, pAB5 [*Ptdc-1*::mCherry] (15 ng/µl) was injected into the LX1832 *lite-1(ce314) lin-15(n765ts)* animals along with pLI5EK (50 ng/µl) to generate five independent extrachromosomal transgenes which were used for behavioral assays. One representative transgenic strain, MIA259 [*keyEx48*; *lite-1(ce314) lin-15(n765ts)*], was kept.

VC neurons

Strains MIA144 *keyIs33* and MIA146 *keyIs46* expressing Tetanus Toxin in the VC neurons from the *lin-11* promoter/enhancer have been described (Kopchock *et al.* 2021). To eliminate HSNs in these VC-silenced animals, wild-type N2 males were crossed into MIA26 *egl-1(n986dm) V* hermaphrodites, and the heterozygous *egl-1(n986dm)/+* males were then crossed to MIA146 *keyIs46; lite-1(ce314) lin-15(n765ts) X* hermaphrodites, and the cross-progeny were then selfed, generating the homozygous strain MIA173 *keyIs46; egl-1(n986dm) V; lite-1(ce314) lin-15(n765ts) X*. To test whether synaptic transmission from the VCs was required for the hyperactive egg-laying behavior of $G\alpha_o$ signaling mutants, wild-type N2 males were crossed to MIA227 *vsIs186; vsIs50 lite-1(ce314) lin-15(n765ts) X* hermaphrodites and the resulting heterozygous cross-progeny were then crossed MIA144 hermaphrodites, allowed to self, generating MIA370 *vsIs186; keyIs33; vsIs50 lite-1(ce314) lin-15(n765ts) X*. To test how complete loss of GOA-1 affected egg laying in VC-silenced animals, we crossed wild-type N2 males into DG1856 *goa-1(sa734) I* hermaphrodites, and the heterozygous *goa-1(sa734)/+* cross-progeny were then mated with MIA144 hermaphrodites. The cross-progeny were allowed to self, generating MIA371 *goa-1(sa734) I; keyIs33; lite-1(ce314) lin-15(n765ts) X*. The presence of *goa-1(sa734)* was confirmed by Sanger sequencing.

Fluorescence imaging

Ratiometric Ca^{2+} imaging

Ratiometric Ca^{2+} recordings were performed on freely behaving animals mounted between a glass coverslip and chunk of NGM agar, as previously described (Collins and Koelle 2013; Li *et al.* 2013; Collins *et al.* 2016; Ravi *et al.* 2018b). Briefly, recordings were collected on an inverted Leica TCS SP5 confocal microscope using the 8 kHz resonant scanner at ~20 fps at 256 × 256 pixel resolution, 12-bit depth and ≥2X digital zoom using a 20x Apochromat objective (0.7 NA) with the pinhole opened to ~20 µm. GCaMP5G and mCherry fluorescence was excited using a 488 nm and

561 nm laser lines, respectively. Adult recordings were performed 24 hours after the late L4 stage. After staging, animals were allowed to adapt for ~30 minutes before imaging. During imaging, the stage and focus were adjusted manually to keep the relevant cell/pre-synapse in view and in focus.

Ratiometric analysis (GCaMP5: mCherry) for all Ca^{2+} recordings was performed after background subtraction using Volocity 6.3.1 as described (Ravi *et al.* 2018a). The egg-laying active state was operationally defined as the period one minute prior to the first egg-laying event and ending one minute after the last (in the case of a typical active phase where 3–4 eggs are laid in quick succession). However, in cases where two egg-laying events were apart by >60 s, peaks were considered to be in separate active phases and any transients observed between were considered to be from an inactive state. In animals where we observed no Ca^{2+} peaks during the entire recording, the total duration of the recording was considered as one, long, inter-transient interval. In animals where we observed a single Ca^{2+} transient, the duration from the start of the recording to the time of the Ca^{2+} transient and the time from the Ca^{2+} transient to the end of the recording were defined as inter-transient intervals. Animals overexpressing NLP-7 become highly egg-laying defective, and the embryonic expression of mCherry from the *nlp-3* promoter in accumulated eggs interfered with the standard image segmentation protocol based on the mCherry channel. For these animals, unambiguous Ca^{2+} transient-dependent changes in GCaMP5 fluorescence localized at the HSN cell body were scored manually, and the frequency of such events were calculated as the number of observed events per unit recording time, typically 10–20 minutes.

Behavior assays and microscopy

Animal sterilization

Animals were sterilized using Floxuridine (FUDR) as described (Mitchell *et al.* 1979; Collins *et al.* 2016; Ravi *et al.* 2018a). Briefly, 100 µl of 10 mg/ml FUDR was applied to OP50 seeded NGM plates. Late L4 animals were then staged onto the FUDR plates, and the treated adults were imaged ~24 hours later.

Egg laying assays

Unlaid eggs were quantitated as described (Chase *et al.* 2004). Staged adults were obtained by picking late L4 animals and culturing them for 30–40 hours at 20°C. The percentage of early-stage eggs laid were quantified as described (Koelle and Horvitz 1996). Thirty staged adults were placed on a thin lawn of OP50 bacteria on a NGM agar plate (Brenner 1974) and allowed to lay eggs for 30 minutes. This was repeated with new sets of staged animals until a total of at least 100 laid eggs were analyzed. Each egg was examined under a Leica M165FC stereomicroscope and categorized into the following categories: eggs which have 1 cell, 2 cell, 3–4 cell, 5–8 cell, and embryos with >8 cells. Eggs with eight cells or fewer were classified as "early stage."

Long-term recording of egg-laying behavior

Egg-laying behavior was recorded at 4–5 frames per second from 24-hour adults after transfer to NGM plates seeded with a thin lawn of OP50 bacterial food using a Leica M165FC stereomicroscope and camera (Grasshopper 3, 4.1 Megapixel, USB3 CMOS camera, Point Grey Research). N2 wild-type and hyperactive egg-laying mutant strains (MT2426 and LX850) were recorded for 3 hours, and the egg-laying defective strains MT8504 and LX849 were recorded for 8–10 hours. Average duration of active and inactive states from these recordings were calculated as described (Waggoner *et al.* 1998, 2000).

Electrophysiology

Electrophysiological recordings were carried out on an upright microscope (Olympus BX51WI) coupled with an EPC-10 amplifier and Patchmaster software (HEKA), as previously described (Yue *et al.* 2018; Zou *et al.* 2018). Briefly, day 2 adult worms were glued on the surface of Sylgard-coated coverslips using the cyanoacrylate-based glue (Gluture Topical Tissue Adhesive, Abbott Laboratories). A dorsolateral incision was made using a sharp glass pipette to expose the cell bodies of HSN neurons for recording. The bath solution contained (in mM) 145 NaCl, 2.5 KCl, 5 $CaCl_2$, 1 $MgCl_2$, and 20 glucose (325–335 mOsm, pH adjusted to 7.3). The pipette solution contained (in mM) 145 KCl, 5 $MgCl_2$, 5 EGTA, 0.25 $CaCl_2$, 10 HEPES, 10 glucose, 5 Na_2ATP and 0.5 NaGTP (315–325 mOsm, pH adjusted to 7.2). The resting membrane potentials were tested with 0 pA holding under the Current Clamp model of the whole-cell patch. The high Cl^- content of the intracellular solution used may contribute to the relatively depolarized membrane potentials we observed (Liu *et al.* 2018).

Experimental design and statistical analysis

Sample sizes for behavioral assays followed previous studies (Chase *et al.* 2004; Collins and Koelle 2013; Collins *et al.* 2016). No explicit power analysis was performed before the study. Statistical analysis was performed using Prism v.6-8 (GraphPad). Behavior experiments were typically performed at least twice on separate days. Ca^{2+} transient peak amplitudes and inter-transient intervals were pooled from data collected from multiple animals over several days (typically ~10 animals recorded per genotype/condition per experiment with ~2–3 recordings obtained per genotype per recording session). No animals or data were excluded. Individual *P*-values are indicated in each Figure legend, and all tests were corrected for multiple comparisons (Bonferroni for ANOVA and Fisher exact test; Dunn for Kruskal-Wallis). For clarity, data not expected (or shown) to be normally distributed are presented in cumulative distribution plots rather than standard scatterplots.

Data availability

The authors affirm that all data necessary for confirming the conclusions of this article are represented fully within the article and its tables and figures. Requests for strains, plasmids, and ratiometric fluorescence recordings used to generate Ca^{2+} traces can be directed to KMC. Supplementary material is available at figshare: https://doi.org/10.25386/genetics.14627469.

Results

Reduced inhibitory $G\alpha_o$ signaling leads to premature egg laying and decreases the duration of egg-laying inactive states

To better understand how inhibitory $G\alpha_o$ signaling contributes to egg-laying behavior state transitions, we used mutants and transgenes to manipulate $G\alpha_o$ signaling in specific cells of the egg-laying circuit and analyzed the consequences on cell Ca^{2+} activity and behavior. We found that $G\alpha_o$ signaling inhibits the onset of egg laying. We performed a "time to first egg lay" assay in wild-type animals and in mutants with excessive or reduced $G\alpha_o$ signaling. As previously shown, wild-type animals release their first embryo ~6–7 hours after becoming adults (McMullen *et al.* 2012; Ravi *et al.* 2018a). Animals bearing $G\alpha_o$ loss-of-function or

Table 2 Egg-laying behavior measurements in animals with altered $G\alpha_o$ signaling

Genotype	Intra-cluster interval ($1/\lambda_1$) Average (min) (95%CI range)	Inter-cluster interval ($1/\lambda_2$) Average (min) (95%CI range)	Eggs laid per active state Average ± 95%CI	Unlaid eggs per animal Average ± 95%CI
Wild type	0.42 (0.33–0.51)	22.11 (21.19–23.09)	2.5 ± 0.5	15.9 ± 1.5
goa-1(n1134)	1.31 (0.94–1.67)	12.88* (12.31–12.75)	1.2 ± 0.1‡	2.2 ± 0.3
HSN::Pertussis Toxin	1.69 (1.17–2.20)	12.42* (12.09–12.75)	1.1 ± 0.07‡	5.0 ± 0.4
egl-10(md176)	0.64 (0.49–0.79)	258.6* (231.26–293.42)	2.5 ± 0.2	45.9 ± 3.3
HSN::GOA-1^{Q205L}	0.35 (0.24–0.47)	66.97* (64.14–70.02)	2.2 ± 0.2	36.8 ± 3.8

Long-term behavior recordings were used to extract features of egg-laying active and inactive behavior states for the indicated genotypes, as described (Waggoner *et al.* 1998). "*" indicates significant differences compared to wild-type animals ($P < 0.0001$, Kruskal-Wallis test with Dunn's correction for multiple comparisons), "‡" indicates significant differences compared to wildtype ($P < 0.0001$, one-way ANOVA with Bonferroni correction).

null mutations laid their eggs much earlier, 3–4 hours after becoming adults (Figure 1B). *goa-1(n1134)*, a hypomorphic mutant predicted to lack the conserved N-terminal myristoylation and palmitoylation sequence, and *goa-1(sa734)*, an early stop mutant predicted to be a molecular null (Segalat *et al.* 1995; Robatzek and Thomas 2000), showed similarly precocious onset of egg laying (Figure 1B). This phenotype was shared in transgenic animals where $G\alpha_o$ function was inhibited just in HSNs through the cell-specific expression of Pertussis Toxin (Tanis *et al.* 2008). Because the timing of this first egg-laying event requires serotonin along with HSN function and activity (Ravi *et al.* 2018a), these results suggest that $G\alpha_o$ normally signals in HSN to inhibit neurotransmitter release and thereby delay the first egg-laying active state (Figure 1B). To test the effects of increased $G\alpha_o$ signaling, we analyzed the behavior of *egl-10(md176)* mutants which lack the major RGS protein that terminates $G\alpha_o$ signaling by promoting $G\alpha_o$ GTP hydrolysis (Koelle and Horvitz 1996). *egl-10(md176)* mutants showed a strong and significant delay in the onset of egg laying, laying their first egg ~15 hours after reaching adulthood (Figure 1B). This delay of egg-laying phenotype was shared in transgenic animals expressing the constitutively active $G\alpha_o$ (Q205L) mutant specifically in the HSNs (Tanis *et al.* 2008) and resembled animals developmentally lacking HSNs (Ravi *et al.* 2018a), consistent with $G\alpha_o$ signaling in HSN to inhibit neurotransmitter release that normally drives the onset of egg laying.

To understand how $G\alpha_o$ signaling controls the normal two-state pattern of egg laying, we performed long-term recordings of adults as they transitioned into and out of the active states in which clusters of several eggs are typically laid. We defined intra-cluster intervals as the time elapsed between consecutive egg-laying events within a single active state (*e.g.*, intervals <4 minutes) and inter-cluster intervals as the time elapsed between different active states (*e.g.*, intervals >4 minutes), as described (Waggoner *et al.* 1998; Collins and Koelle 2013). As expected, wild-type animals displayed a two-state pattern of egg laying with multiple egg-laying events clustered within brief, ~2-minute active states about every 20–30 minutes (Figure 1C and Table 2). Animals bearing the *goa-1(n1134)* hypomorphic mutation entered active states two- to threefold more frequently, often laying single eggs during active states separated by only ~12–13 minutes (Figure 1C and Table 2), as previously shown (Waggoner *et al.* 2000). We found the duration of inactive states in animals expressing Pertussis Toxin in the HSN neurons was indistinguishable from the *goa-1(n1134)* mutant, indicating that $G\alpha_o$ signals in HSN to reduce the probability of entering the active state (Figure 1C and Table 2). $G\alpha_o$ is likely the only major target for Pertussis Toxin in the HSNs regulating egg laying, as transgenic re-expression of GOA-1^{Q205L} from an HSN-specific promoter rescues the hyperactive egg-laying defect of Pertussis Toxin expressing animals (Figure 1D). This rescue was qualitatively similar to that seen when GOA-1^{Q205L} was expressed in HSNs of *goa-1(n1134)* mutant animals (Tanis *et al.* 2008). Loss of inhibitory $G\alpha_o$ signaling led to active states in which 1-2 embryos were laid almost immediately after they were positioned in the uterus next to the vulval opening. As a result, successive egg-laying events were often rate-limited by egg production, explaining why the average intra-cluster intervals were typically double that seen in wild-type animals (Figure 1C and Table 2). Indeed, *goa-1* null mutants including *goa-1(sa734)* have a strongly reduced brood size (36 progeny) compared to *goa-1(n1134)* hypomorphic mutants (150 progeny) (Segalat *et al.* 1995), making quantitative measures of intra- and inter-cluster intervals in such mutants challenging. However, analyzing the timing of egg-laying events in animals with too much $G\alpha_o$ signaling supports our interpretation that $G\alpha_o$ does not play a significant role in regulating the timing of egg laying within the active state. Both *egl-10(md176)* mutants with a global increase of $G\alpha_o$ signaling or transgenic animals expressing the $G\alpha_o$(Q205L) mutant specifically in HSNs show the same intra-cluster time constant as wild-type animals (Table 2). In contrast, both *egl-10(md176)* mutant animals or $G\alpha_o$(Q205L) gain-of-function mutation in the HSNs showed prolonged inactive periods of 258 and 67 minutes, respectively (Figure 1C and Table 2), resembling animals lacking HSNs altogether (Waggoner *et al.* 2000). Interestingly, animals without HSNs (Waggoner *et al.* 1998) or with too much inhibitory $G\alpha_o$ signaling (Figure 1C and Table 2) still lay multiple eggs within discrete active states, consistent with our results showing that a stretch-dependent homeostat can maintain the active state even when neurotransmitter release from the HSN is inhibited (Collins *et al.* 2016; Ravi *et al.* 2018a). These results support a model where $G\alpha_o$ signaling in HSN does not modulate patterns of egg laying within active states. Instead, $G\alpha_o$ acts to depress entry into the egg-laying active state.

$G\alpha_o$ signaling inhibits HSN Ca^{2+} activity to promote the inactive behavior state

Previous work has shown that $G\alpha_o$ signals to depress neurotransmitter release (Miller *et al.* 1999; Nurrish *et al.* 1999). Whether $G\alpha_o$

signals to inhibit HSN electrical excitability that might be evident in changes in cell Ca^{2+} activity, or instead signals downstream of Ca^{2+} to regulate steps in UNC-13-dependent docking, priming, and vesicle fusion, has not been tested directly. To address how $G\alpha_o$ signals to inhibit HSN neurotransmitter release, we performed ratiometric Ca^{2+} imaging in our panel of $G\alpha_o$ signaling mutants as they entered spontaneous egg-laying active states. Freely behaving animals bearing the *goa-1(n1134)* hypomorphic or *goa-1(sa734)* null mutations showed a clear change in HSN Ca^{2+} activity from two-state burst firing to more tonic firing (Figure 2A, Supplementary Videos S1–S3). Complete loss of inhibitory $G\alpha_o$ signaling caused a significant increase in the frequency of HSN Ca^{2+} transients (Figure 2, B and C). We were surprised that the *goa-1(n1134)* mutants, which show strongly hyperactive egg-laying behavior indistinguishable from that of *goa-1(sa734)* null mutants, showed only a modest and statistically insignificant increase in HSN Ca^{2+} activity compared to wild-type (Figure 2C). However, our results with *goa-1(n1134)* match previous findings (Shyn *et al.* 2003). The *goa-1(n1134)* hypomorphic mutant is expected to have residual $G\alpha_o$ signaling activity in that its major defect is the absence of a proper membrane anchor sequence (Mumby *et al.* 1990). These results show that $G\alpha_o$ signaling depresses HSN presynaptic activity, but that the hyperactive egg-laying phenotypes observed in *goa-1(n1134)* mutants are not a result of dramatic changes in presynaptic HSN Ca^{2+} activity.

We next tested how increased inhibitory $G\alpha_o$ signaling affects HSN activity. Both *egl-10(md176)* mutants and transgenic animals expressing the activated GOA-1(Q205L) in HSNs showed a significant and dramatic reduction in the frequency of HSN Ca^{2+} transients, with single HSN Ca^{2+} transients occurring several minutes apart (Figure 2, A and B). The rare egg-laying events seen in animals with increased $G\alpha_o$ signaling mostly followed single HSN Ca^{2+} transients, not multi-transient bursts typically seen in wild-type animals (Figure 2, A and C). In one *egl-10(md176)* animal, we observed an egg-laying event that was not accompanied by an HSN Ca^{2+} transient. This suggests that elevated $G\alpha_o$ signaling is sufficient to silence the HSNs, and that, in this case, egg laying becomes HSN-independent. In support of this model, previous work has shown that *egl-10(md176)* mutants respond to serotonin but are resistant to the serotonin reuptake inhibitor imipramine (Trent *et al.* 1983). Alternatively, (or additionally) $G\alpha_o$ signaling may function to depress coordinated activity between the gap-junctioned, contralateral HSNs, whose Ca^{2+} activity we were unable to observe simultaneously because our confocal imaging conditions only captures one HSN at a time.

To determine how disruption of inhibitory $G\alpha_o$ signaling in HSN affects its activity, we recorded HSN Ca^{2+} transients in transgenic animals expressing Pertussis Toxin in the HSNs. $G\alpha_o$-silenced HSNs showed a dramatic increase in the frequency of HSN Ca^{2+} transients, leading to a nearly constitutive, tonic Ca^{2+} activity like that observed in *goa-1(sa734)* null mutants (Figure 3, A–C; Supplementary Video S4). While control animals showed an average HSN Ca^{2+} transient frequency of about ~0.4 transients per minute, animals expressing Pertussis Toxin in HSN showed an average 1.9 transients per minute, a significant increase (Figure 3C). These results suggest that even under normal growth conditions, unidentified neuromodulators signal through $G\alpha_o$-coupled receptors on HSN to inhibit Ca^{2+} activity.

We have previously shown that burst Ca^{2+} activity in the command HSN neurons is initiated and sustained by a stretch-dependent homeostat. In chemically or genetically sterilized animals, burst Ca^{2+} activity in HSN is largely eliminated (Ravi *et al.* 2018a). As such, we were surprised to observe high frequency Ca^{2+} transients in animals with reduced $G\alpha_o$ signaling because these animals typically retain few (1 to 3) eggs in the uterus at steady state, conditions that normally eliminate HSN burst firing. We hypothesized that the stretch-dependent homeostat was not required to promote HSN Ca^{2+} activity in $G\alpha_o$ signaling mutants. To test this, we chemically sterilized transgenic animals expressing Pertussis Toxin in the HSNs with Floxuridine (FUDR), a blocker of

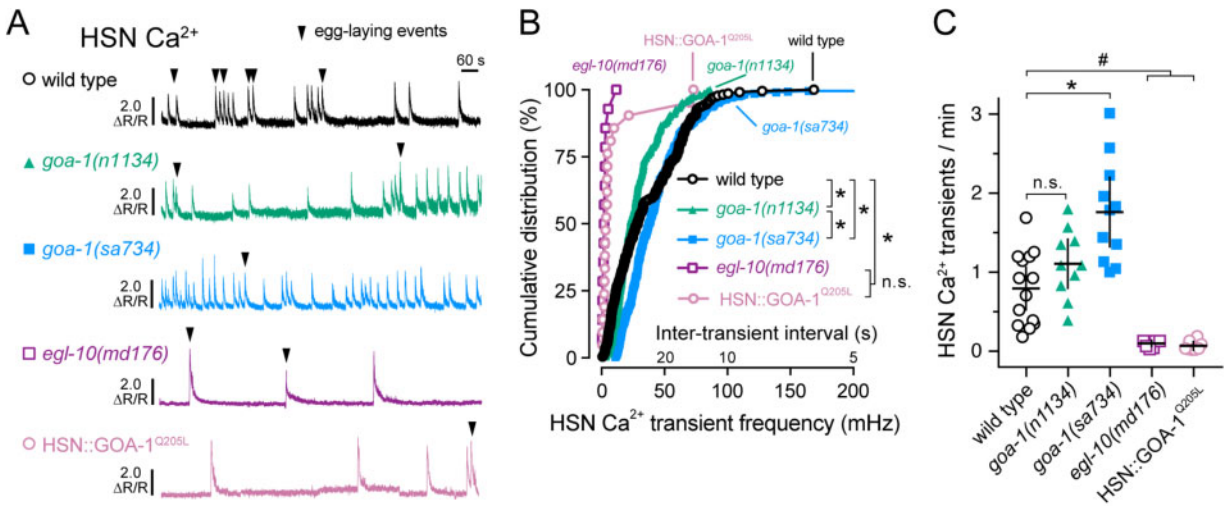

Figure 2 $G\alpha_o$ signaling inhibits HSN neuron Ca^{2+} activity and burst firing. (A) Representative GCaMP5: mCherry (ΔR/R) ratio traces showing HSN Ca^{2+} activity in freely behaving wild-type (black), *goa-1(n1134)* loss-of-function mutant (green), *goa-1(sa734)* null mutant (blue), and *egl-10(md176)* null (purple) mutant animals, along with transgenic animals expressing the activated GOA-1(Q205L) in the HSN neurons (pink) during an egg-laying active state. Arrowheads indicate egg-laying events. (B) Cumulative distribution plots of instantaneous Ca^{2+} transient peak frequencies (and inter-transient intervals) in wild-type (black open circles), *goa-1(n1134)* (green filled triangles), *goa-1(sa734)* (blue squares), *egl-10(md176)* mutants (purple open squares) along with transgenic animals expressing the activated GOA-1(Q205L) in the HSN neurons (pink open circles). Asterisks indicate $P < 0.0001$ (Kruskal-Wallis test with Dunn's correction for multiple comparisons). (C) Scatter plots show average Ca^{2+} transient frequency (per min). Error bars indicate 95% confidence intervals for the mean. Asterisk indicates $P < 0.0001$; pound (#) indicates $P \leq 0.0079$; n.s. indicates $P > 0.05$ (one-way ANOVA with Bonferroni correction for multiple comparisons).

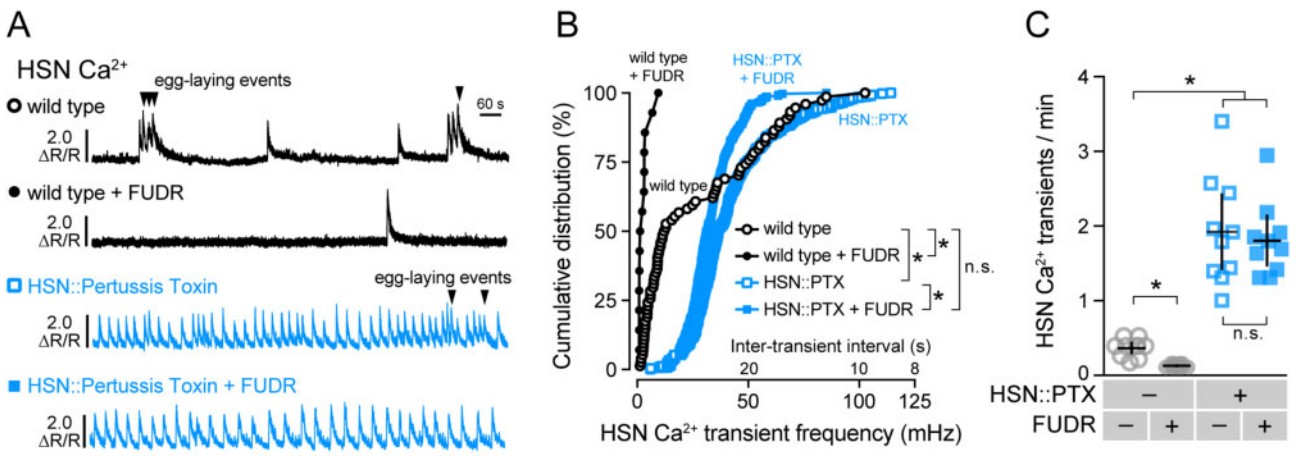

Figure 3 Inhibitory $G\alpha_o$ signaling in HSN is required for two-state Ca^{2+} activity and facilitates modulation by feedback of egg accumulation. (A) Representative GCaMP5: mCherry (ΔR/R) ratio traces showing HSN Ca^{2+} activity in untreated (fertile) wild-type animals (black open circles), FUDR-sterilized wild-type animals (black filled circles), untreated (fertile) animals expressing Pertussis Toxin (PTX) in the HSN neurons (blue open squares), and in FUDR-sterilized transgenic animals expressing PTX in the HSNs (blue filled squares). Arrowheads indicate egg-laying events. (B) Cumulative distribution plots of instantaneous Ca^{2+} transient peak frequencies (and inter-transient intervals) in untreated and FUDR-treated animals. Asterisks indicate $P < 0.0001$ (Kruskal-Wallis test with Dunn's test for multiple comparisons). (C) Scatter plots show average Ca^{2+} transient frequency (per min). Error bars indicate 95% confidence intervals for the mean. Asterisks indicate $P < 0.0001$ (one-way ANOVA with Bonferroni's test for multiple comparisons). Data from 10 animals were used for each strain for analysis.

embryogenesis (Mitchell *et al.* 1979), and recorded HSN Ca^{2+} activity. Wild-type animals treated with FUDR showed a dramatic decrease in the frequency of HSN Ca^{2+} activity and an elimination of burst firing (Figure 3, A–C), as we have previously shown (Ravi *et al.* 2018a). Sterilized transgenic animals expressing Pertussis Toxin in the HSNs showed only a slight reduction in HSN Ca^{2+} frequency (Figure 3, A and B). Both fertile and sterile Pertussis Toxin-expressing animals had dramatically and significantly increased HSN Ca^{2+} transient frequency (~1.9/minute), indicating their HSNs no longer responded to the retrograde signals of egg accumulation arising from the stretch-homeostat. One explanation for this result could be that in fertile wild-type animals, feedback of egg accumulation elevates HSN excitability above a firing threshold that overcomes endogenous inhibitory $G\alpha_o$ signaling. Together, these results support a model where $G\alpha_o$ signals in HSN to depress cell electrical excitability which allows for the proper two-state pattern of HSN Ca^{2+} activity that responds to homeostatic feedback of egg accumulation.

Presynaptic $G\alpha_o$ signaling inhibits postsynaptic vulval muscle activity

To test how changes in inhibitory $G\alpha_o$ signaling affect the postsynaptic vulval muscles, we recorded Ca^{2+} activity in the vulval muscles of *goa-1(n1134)* mutant and Pertussis Toxin expressing transgenic animals. Both wild-type and *goa-1(n1134)* mutants showed increased vulval muscle Ca^{2+} transients as the animals entered the egg-laying active state (Figure 4, A and B). *goa-1(n1134)* mutants also showed elevated muscle activity compared to wild-type control animals during inactive states when no eggs were laid (Figure 4, A and B), as previously shown (Shyn *et al.* 2003). Surprisingly, Ca^{2+} activity during egg-laying active states was not significantly different in *goa-1(n1134)* mutant animals (Figure 4, A and B; compare Supplementary Videos S5 and S6), a result consistent with $G\alpha_o$ signaling primarily to prolong the inactive state. These results suggest $G\alpha_o$ signals to inhibit circuit activity during the egg-laying inactive state and/or that loss of $G\alpha_o$ elevates circuit activity that prolongs the active state beyond the brief ~2–3 minutes window during which eggs are typically laid (Waggoner *et al.* 1998). Recordings of vulval muscle Ca^{2+} activity in transgenic animals expressing Pertussis Toxin in the presynaptic HSNs show a dramatic and significant increase in vulval muscle Ca^{2+} transient frequency during both active and inactive states (Figure 4, C and D; Supplementary Video S7), confirming $G\alpha_o$ is required in HSN to inhibit neurotransmitter release.

We have previously shown that egg accumulation promotes vulval muscle excitability during the active state while sterilization reduces it to that seen during the inactive state (Collins *et al.* 2016; Ravi *et al.* 2018a). Because FUDR-sterilization failed to reduce HSN Ca^{2+} activity in Pertussis Toxin expressing animals (Figure 3C), we predicted that vulval muscle Ca^{2+} activity would remain similarly elevated in these animals after sterilization. To our surprise, FUDR treatment significantly reduced, but did not completely eliminate, the elevated vulval muscle Ca^{2+} activity in animals expressing Pertussis Toxin in HSN (Figure 4, C and D). This result suggests egg accumulation and/or germline activity is still required for full vulval muscle activity even when HSN Ca^{2+} activity is dramatically increased. However, because these animals lay eggs almost as soon as they are made, the degree of uterine stretch necessary to induce the active state must be markedly reduced. This supports a model where both the stretch-dependent homeostat and $G\alpha_o$ signaling dynamically interact to regulate egg-laying behavior states.

$G\alpha_o$ signaling modulates the HSN resting membrane potential

Reduction of inhibitory $G\alpha_o$ signaling strongly increased HSN Ca^{2+} activity and burst firing, prompting us to investigate whether $G\alpha_o$ signals to modulate HSN electrical excitability. We recorded the resting membrane potential of the HSN neurons in animals with altered $G\alpha_o$ signaling using the whole-cell patch clamp technique (Figure 5A), as described (Yue *et al.* 2018). As shown in Figure 5B, transgenic animals expressing Pertussis Toxin specifically in the HSNs had significantly depolarized HSNs (−14.75 mV) compared to the wild-type parental strain (−21.8 mV). Similarly, hypomorphic *goa-1(n1134)* loss-of-function mutants had more depolarized resting potentials (−17.9 mV) compared to HSNs from recorded wild-type animals (−21.1 mV). In contrast, the resting membrane potential of HSNs in *egl-*

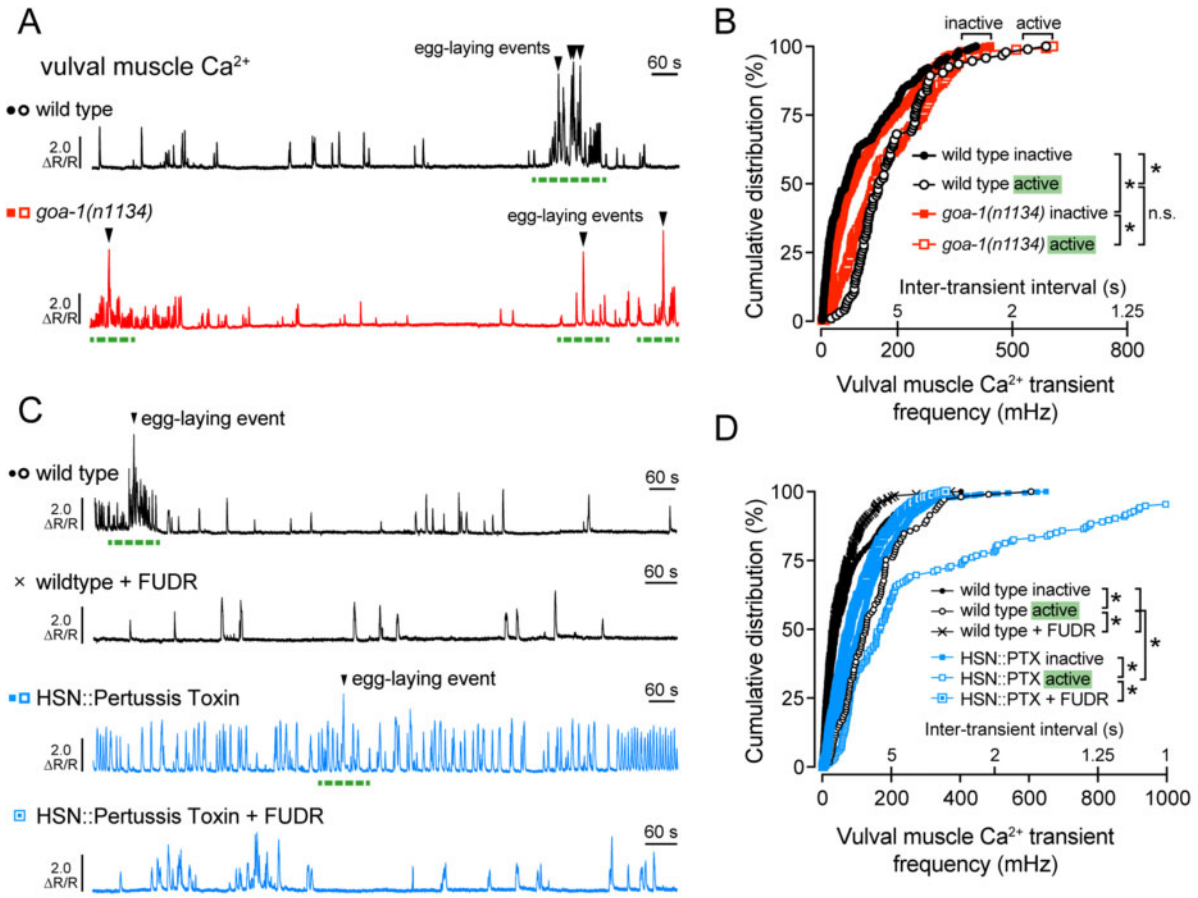

Figure 4 $G\alpha_o$ signals in HSN to reduce excitatory modulation of the vulval muscles. (A) Representative GCaMP5: mCherry (ΔR/R) ratio traces showing vulval muscle Ca^{2+} activity in wild-type (black) and *goa-1(n1134)* loss-of-function mutant animals (red). Egg-laying events are indicated by arrowheads, and egg-laying active states are indicated by dashed green lines. (B) Cumulative distribution plots of instantaneous vulval muscle Ca^{2+} transient peak frequencies (and inter-transient intervals) in wild-type (black circles) and *goa-1(n1134)* mutant animals (red squares) in the inactive and active egg-laying states (filled and open, respectively). (C) Representative GCaMP5: mCherry (ΔR/R) ratio traces showing vulval muscle Ca^{2+} activity in untreated (circles) and FUDR-treated (cross) wild-type animals (black) along with untreated (filled) or FUDR-treated (open) transgenic animals expressing Pertussis Toxin in the HSNs (blue squares). Egg-laying events are indicated by arrowheads, and egg-laying active states are indicated by green dashed lines. (D) Cumulative distribution plots of instantaneous vulval muscle Ca^{2+} transient peak frequencies (and inter-transient intervals) in wildtype and in transgenic animals expressing Pertussis Toxin in the HSN neurons, with or without FUDR treatment (black cross or blue square), during the inactive and active egg-laying states (filled and open, respectively). Asterisks indicate $P < 0.0001$ (Kruskal-Wallis test with Dunn's test for multiple comparisons).

10(md176) $G\alpha_o$ RGS protein mutant animals with a global increase in $G\alpha_o$ signaling (Koelle and Horvitz 1996) was significantly hyperpolarized (−40.8 mV) compared to wild-type control animals (Figure 5B). To confirm this hyperpolarization arose from changes in $G\alpha_o$ signaling in HSN, we transgenically expressed EGL-10 from cDNA in the HSNs of *egl-10(md176)* mutant animals. Re-expression of EGL-10 raised the membrane potential to −18.7 mV from −30.4 mV. The hyperpolarization of HSNs in *egl-10(md176)* mutants explains the reduced frequency of HSN Ca^{2+} transients and their strong defects in egg-laying behavior. These results show that $G\alpha_o$ signals in the HSNs to promote membrane polarization, reducing cell electrical excitability, Ca^{2+} activity, and neurotransmitter release.

Inhibition of egg laying by $G\alpha_o$ is not replicated by elevated βγ expression

Receptor activation of $G\alpha_{i/o}$ heterotrimers releases βγ subunits which have previously been shown to bind to activate specific K^+ channels and inhibit Ca^{2+} channels (Reuveny *et al.* 1994; Herlitze *et al.* 1996). RNAi-mediated knockdown of the GPB-1 β subunit in HSN reduces egg-laying behavior (Esposito *et al.* 2007). An increase in free βγ subunits in $G\alpha_o$ mutants might explain their hyperactive egg-laying behavior phenotypes. To test if βγ over-expression in HSN would increase egg laying, we transgenically overexpressed the sole nonRGS Gβ subunit, GPB-1 (Jansen *et al.* 1999), and the broadly expressed Gγ subunit, GPC-2 (Yamada *et al.* 2009), under the *tph-1* promoter along with GFP. βγ over-expression in HSN did not cause any significant differences in steady-state egg accumulation (Figure 5C). The number of eggs stored *in-utero* in these animals (13.0 ± 1.1 eggs) was comparable to wild-type animals (15.7 ± 1.2 eggs) and less than *egl-10(md176)* mutant animals (44.5 ± 2.3 eggs). These results suggest that $G\alpha_o$ signals to inhibit HSN activity in a distinct manner from simple titration or release of βγ subunits.

Egg-laying behavior is dysregulated in cAMP and cGMP signaling mutants

$G\alpha_o$ is in the $G\alpha_{i/o}$ class of G proteins that bind to and inhibit nucleotide cyclases, which function to reduce cAMP and cGMP levels and their subsequent activation of protein kinases (Kobayashi

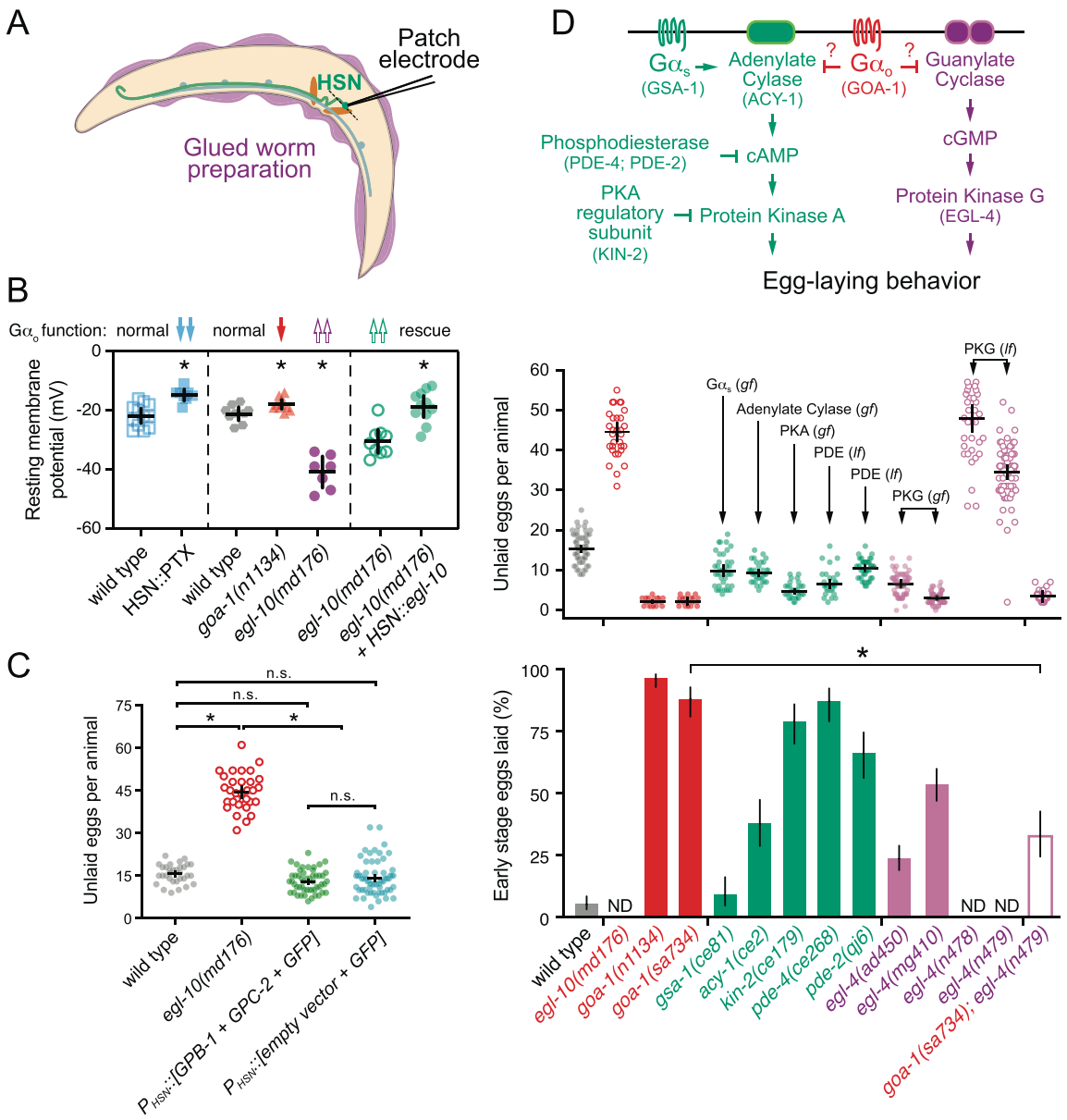

Figure 5 $G\alpha_o$ signaling depresses HSN resting membrane potential and may inhibit egg-laying behavior in parallel to βγ, cGMP, and cAMP signaling pathways. (A) Cartoon of the glued worm preparation used for patch clamp electrophysiology of HSN. (B) Scatter plots show resting membrane potentials in (left) transgenic animals expressing either nothing (blue open squares) or Pertussis Toxin in HSN (blue filled squares). Asterisk indicates $P < 0.0001$ (Student's *t*-test). (center) Resting membrane potentials of wild-type control animals (grey hexagons), *goa-1(n1134)* loss-of-function mutants (red triangles), and *egl-10(md176)* null mutants (purple filled circles). Asterisks indicate $P \leq 0.0347$ (one-way ANOVA with Bonferroni correction for multiple comparisons). (right) Resting membrane potentials in transgenic *egl-10(md176)* animals expressing in HSN either GFP alone (green open circles) or GFP + *egl-10* cDNA driven by the HSN-specific *tph-1* promoter (green filled circles). Asterisks indicate $P < 0.0001$ (Student's *t*-test). Error bars indicate 95% confidence intervals for the mean. $N \geq 7$ animals recorded per genotype. (C) Scatter plots show average number of eggs retained by wild-type animals (gray filled circles), *egl-10(md176)* null mutants (orange open circles), and in transgenic animals expressing either Gβ (GPB-2) and Gγ (GPC-1) subunits (green filled circles) or nothing (blue filled circles) in HSN from the *tph-1* gene promoter along with GFP. Error bars indicate means with 95% confidence intervals. Asterisk indicates $P < 0.0001$; n.s. indicates $P > 0.05$ (one-way ANOVA with Bonferroni correction for multiple corrections). (D) Top, cartoon of how $G\alpha_o$ signaling might interact with cAMP and cGMP signaling pathways. Gene names for *C. elegans* orthologs tested here are indicated in parentheses. Middle, scatterplots show average number of eggs retained by wildtype (grey), *egl-10(md176)* (red open circles), *goa-1(n1134)* and *goa-1(sa734)* $G\alpha_o$ loss of function (red filled circles) mutants, and in animals with altered cAMP effector signaling (green): *gsa-1(ce81)* $G\alpha_s$ gain-of-function, *acy-1(ce2)* Adenylate Cyclase gain-of-function, *kin-2(ce179)* protein kinase A (PKA) inhibitory regulatory subunit loss-of-function, *pde-4(ce268)* Phosphodiesterase (PDE) loss-of-function, *pde-2(qj6)* Phosphodiesterase (PDE) null; altered cGMP effector signaling (pink): *egl-4(ad805)* and *egl-4(mg410)* protein kinase G (PKG) gain-of-function (pink filled circles), *egl-4(n478)* and *egl-4(n479)* loss-of-function mutants (pink open circles). Mean totals below ~10 eggs indicate hyperactive egg laying while totals above ~20 eggs indicate egg-laying behavior defects. Bottom, bar graphs indicate percent of embryos laid at early stages of development. Animals laying ≥50% embryos at early stages are considered hyperactive. Error bars indicate ± 95% confidence intervals for the mean proportion. N.D. indicates the stages of eggs laid was not determined because those mutants are egg-laying defective (Egl). Asterisk indicates highlighted significant differences ($P \leq 0.0001$; Fisher Exact Test with Bonferroni correction for multiple comparisons).

et al. 1990; Zhang and Pratt 1996; Matsubara 2002; Ghil et al. 2006). The hyperactive egg-laying behavior phenotypes of animals with reduced $G\alpha_o$ function could be explained by a failure to properly terminate cAMP and/or cGMP signaling (Figure 5D, top). To test this, we analyzed egg-laying behavior in strains bearing mutations that increase $G\alpha_s$ and cAMP effector signaling (Reynolds et al. 2005; Schade et al. 2005; Charlie et al. 2006a, 2006b). Animals carrying *gsa-1(ce81)* gain-of-function mutations in $G\alpha_s$ are predicted to increase signaling accumulate fewer eggs compared to wild-type animals (Figure 5D, middle). Because a reduction in steady-state egg accumulation could be caused by indirect effects of these mutations on egg production or brood size, we also examined the developmental age of embryos laid. As previously reported (Bany et al. 2003), loss of inhibitory $G\alpha_o$ signaling causes embryos to be laid precociously, before they reach the 8-cell stage (Figure 5D, bottom). $G\alpha_s$ gain-of-function mutant animals do not show a corresponding increase in early-stage embryos that are laid, suggesting the reduction in egg accumulation observed in $G\alpha_s$ gain-of-function mutant animals is indirect. In contrast, gain-of-function *acy-1* Adenylate Cyclase mutations or loss-of-function *pde-4* phosphodiesterase mutations, both predicted to result in increased cAMP signaling, cause animals to accumulate fewer eggs and lay them at earlier stages (Figure 5D). Similarly, *kin-2* mutations that disrupt an inhibitory regulatory subunit of protein kinase A showed a modest but significant hyperactive egg-laying phenotype. Together, these results indicate that $G\alpha_s$, cAMP, and protein kinase A signaling promote egg-laying behavior. Because these mutant phenotypes were not nearly as strong as animals carrying $G\alpha_o$ mutants, $G\alpha_o$ likely signals to inhibit egg laying via other effectors.

Extensive work has shown that the cGMP-dependent protein kinase G, EGL-4, regulates egg laying in *C. elegans* (Fujiwara et al. 2002; L'Etoile et al. 2002; Raizen et al. 2006; Hao et al. 2011). Mutations which increase EGL-4 activity cause hyperactive egg laying and release of early stage embryos, while elimination of EGL-4 signaling causes egg-laying defects and significant egg accumulation (Figure 5D, middle). To determine whether $G\alpha_o$ and protein kinase G regulate egg laying in a shared pathway, we performed a genetic epistasis experiment. *goa-1(sa734); egl-4(n479)* double null mutants accumulate very few eggs (Figure 5D, middle), resembling the *goa-1(sa734)* null mutant. However, the low brood size of the *goa-1(sa734)* mutant could prevent accurate measurement of these animal's egg-laying defects. To address this, we measured the stage of eggs laid as indicated above. Loss of the EGL-4 protein kinase G strongly and significantly suppressed the hyperactive egg-laying behavior of $G\alpha_o$ null mutants (Figure 5D, bottom). *goa-1(sa734); egl-4(n479)* mutants laid 33% of their embryos at early stages compared to 88% for the *goa-1(sa734)* single mutant, an intermediate egg-laying phenotype. These results are consistent with cGMP and/or protein kinase G signaling acting downstream of or parallel to $G\alpha_o$ in the proper regulation of egg-laying behavior, but their precise relationship remains unclear at this point.

$G\alpha_o$ signals in the vulval muscles and uv1 neuroendocrine cells to inhibit egg laying

In addition to HSN, GOA-1 is expressed in all neurons of the reproductive circuit, the egg-laying vulval muscles, and the uv1 neuroendocrine cells (Mendel et al. 1995; Segalat et al. 1995; Jose et al. 2007), raising questions as to how $G\alpha_o$ signaling functions in those other cells to regulate egg-laying behavior. Previous work has shown that GOA-1(Q205L) was sufficient to rescue the hyperactive egg-laying behavior of *goa-1(n1134)* mutants when expressed in the HSNs but had little effect when expressed in the VCs or vulval muscles (Tanis et al. 2008). Similarly, transgenic expression of Pertussis Toxin in the VCs or vulval muscles failed to modify egg-laying behavior strongly (Tanis et al. 2008). Previous work failing to identify a function for $G\alpha_o$ in the vulval muscles used a modified *Nde*-box element from the *ceh-24* promoter that drives expression more efficiently in the vm1 muscle cells compared to the vm2 muscles innervated by the HSN and VC neurons (data not shown). We find that expression of Pertussis Toxin in both vm1 and vm2 vulval muscles from a larger region of the *ceh-24* gene promoter (Harfe and Fire 1998; Ravi et al. 2018a) also failed to cause any significant changes in the steady-state egg accumulation (Figure 6A). Conversely, expression of the activated GOA-1(Q205L) mutant in the vulval muscles from the same promoter did cause a modest but significant egg-laying defect, with animals accumulating 24.1 ± 2.0 eggs compared to mCherry-expressing control transgenic animals (13.2 ± 0.7 eggs). This egg-laying defect was significantly weaker than *egl-10(md176)* mutants (46.0 ± 3.3 eggs) or transgenic animals expressing GOA-1(Q205L) just in the HSNs (36.8 ± 3.8 eggs). We do not believe this modest egg-laying defect was caused by transgene expression outside of the vulval muscles, as blocking synaptic transmission via transgenic expression of Tetanus Toxin from the same *ceh-24* promoter showed no such egg-laying defect (Figure 6B). Collectively, these results show that $G\alpha_o$ does not play a significant role in suppressing vulval muscle excitability under steady-state conditions but that activated $G\alpha_o$ can signal in these cells to induce a mild but significant inhibition of cell activity and egg-laying behavior.

The uv1 cells express the neurotransmitter tyramine along with NLP-7 and FLP-11 neuropeptides which inhibit egg laying (Alkema et al. 2005; Collins et al. 2016; Banerjee et al. 2017). Based on the function of $G\alpha_o$ signaling in inhibiting neurotransmitter release in neurons, we would expect that loss of $G\alpha_o$ function in uv1 would enhance their excitability, promoting release of inhibitory tyramine and neuropeptides, causing a reduction of egg laying. Surprisingly, previous work has shown that transgenic expression of Pertussis Toxin in uv1 cells increased the frequency of early-stage eggs that are laid, similar to the blocking of neurotransmitter release by Tetanus Toxin (Jose et al. 2007). A caveat of these experiments is that the *ocr-2* gene promoter used for transgene expression in uv1 also expresses in the utse (uterine-seam) associated cells and head sensory neurons (Jose et al. 2007). To test whether $G\alpha_o$ functions specifically in uv1 to regulate egg laying, we used the *tdc-1* gene promoter (Alkema et al. 2005) along with the *ocr-2* 3' untranslated region (Jose et al. 2007) to drive expression more specifically in uv1. Transgenic expression of Pertussis Toxin in uv1 caused a mild but significant decrease in steady-state egg accumulation (10.9 ± 1.5 eggs) compared to mCherry-expressing control animals (15.3 ± 1.2 eggs), indicating $G\alpha_o$ signaling facilitates uv1-dependent inhibition of egg-laying behavior (Figure 6C). We also tested how increased $G\alpha_o$ signaling in uv1 affects egg laying. Transgenic expression of the activated GOA-1(Q205L) mutant in uv1 cells caused no quantitative differences in egg accumulation (15.5 ± 2.1 eggs) (Figure 6C). Together, these results show that $G\alpha_o$ has a limited role in regulating egg-laying behavior in the vulval muscles or uv1 neuroendocrine cells, unlike the strong phenotypes observed when we genetically manipulate $G\alpha_o$ function in HSN.

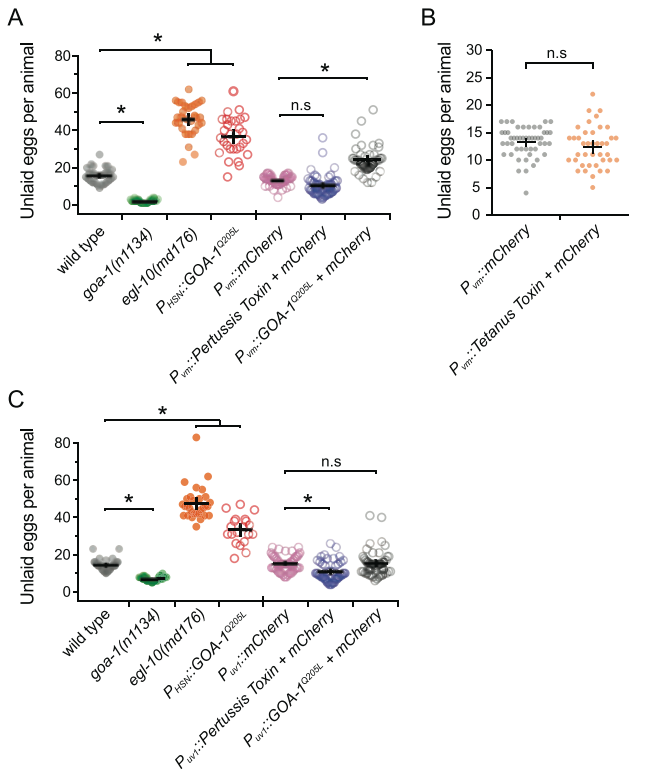

Figure 6 Altered $G\alpha_o$ signaling in the vulval muscles and uv1 neuroendocrine cells causes only modest effects on egg laying. (A) Scatter plots show average number of eggs retained by wild-type (grey), *goa-1(n1134)* mutants (green), *egl-10(md176)* null mutant animals (orange) along with transgenic animals expressing GOA-1^{Q205L} in the HSNs (red open circles) compared to transgenic animals expressing mCherry only (pink open circles), Pertussis Toxin (blue open circles), or GOA-1^{Q205L} (black open circles) in the vulval muscles from the *ceh-24* gene promoter. (B) Scatter plots show average number of eggs retained in transgenic animals expressing mCherry only (gray) or Tetanus Toxin along with mCherry (orange) in the vulval muscles (vm) using the *ceh-24* gene promoter. Error bars indicate means with 95% confidence intervals. (C) Scatter plots show average number of eggs retained by wild-type (grey), *goa-1(n1134)* mutant (green), *egl-10(md176)* null mutant (orange) animals, and transgenic animals expressing GOA-1^{Q205L} in the HSNs (red) compared to transgenic animals expressing mCherry only (pink), Pertussis Toxin (blue), or GOA-1^{Q205L} (black open circles) in the uv1 neuroendocrine cells from the *tdc-1* gene promoter. Four or five independent extrachromosomal arrays were generated for each transgene in (A–C) and ~10 animals bearing each extrachromosomal array were analyzed. Error bars indicate 95% confidence intervals for the mean. Asterisks indicate $P < 0.0001$; n.s. indicates $P > 0.05$ (one-way ANOVA with Bonferroni's correction for multiple comparisons or Student's *t* test).

NLP-7 inhibition of HSN activity and egg-laying requires the EGL-47 receptor and $G\alpha_o$

Multiple neuropeptides and receptors have been identified to inhibit egg laying by signaling through $G\alpha_o$-coupled receptors expressed on HSN (Figure 1A). Recent work has identified NLP-7 neuropeptides, synthesized in the VC neurons and uv1 neuroendocrine cells, as potential ligands for EGL-47 receptor signaling through $G\alpha_o$ (Moresco and Koelle 2004; Banerjee *et al.* 2017). Animals overexpressing the NLP-7 neuropeptide are egg-laying defective, accumulating 39.6 ± 3.4 eggs in the uterus (Figure 7A). To test how NLP-7 inhibits egg laying, we crossed NLP-7 over-expressing transgenes into *goa-1* mutant animals and evaluated their egg-laying behavior phenotypes. As shown in Figure 7A, the hypomorphic *goa-1(n1134)* loss-of-function mutant significantly suppressed these egg-laying defects, as previously shown (Banerjee *et al.* 2017). However, the suppression by *goa-1(n1134)* was incomplete; NLP-7 over-expressing, *goa-1(n1134)* double mutant animals retained more eggs than the *goa-1(n1134)* single mutant (Table 2) or even wild-type control animals (Figure 7A). To confirm whether $G\alpha_o$ was required for NLP-7 inhibition, we tested the *goa-1(sa734)* null mutant and found it fully suppressed the egg-laying defects caused by NLP-7 over-expression. To confirm this epistatic relationship, we measured the stage of embryos laid by these animals. *goa-1(sa734)* null mutant animals over-expressing NLP-7 laid ~100% of their embryos at early stages, a level not significantly different *goa-1(sa734)* single mutant animals (Figure 7B). Together, these results show that NLP-7 neuropeptides cannot inhibit egg-laying behavior in the absence of $G\alpha_o$ function.

Because the HSNs appear to be the principal sites of inhibitory $G\alpha_o$ signaling, we tested how NLP-7 over-expression affects HSN Ca^{2+} activity. As expected, over-expression of NLP-7 strongly inhibited HSN Ca^{2+} activity (Figure 7, C and D), consistent with the strong egg-laying defects of these animals. To our surprise, loss of $G\alpha_o$ in these animals did now show high frequency HSN Ca^{2+} transient activity, despite showing the strong hyperactive egg-laying behavior of *goa-1(sa734)* single mutants (Figure 7, C and D). This result shows that the hyperactive egg-laying behavior of $G\alpha_o$ null mutants is unlinked to the increase in HSN Ca^{2+} activity we observe. Previous work showed NLP-7 inhibition of HSN activity and egg laying requires the EGL-47 receptor (Banerjee *et al.* 2017). To show directly whether NLP-7 inhibition of HSN activity requires the EGL-47 receptor, we recorded HSN Ca^{2+} activity in *egl-47(ok677)* null mutants. Unexpectedly, animals lacking EGL-47 had significantly fewer HSN Ca^{2+} transients than wild-type animals whether or not NLP-7 was over-expressed (Figure 7D). These results show that although NLP-7 signals to silence HSN Ca^{2+} activity, it does not require EGL-47 or $G\alpha_o$ function to do so.

To confirm whether NLP-7 inhibition of egg laying requires EGL-47 and $G\alpha_o$ function outside of HSN, we compared egg-laying behavior in NLP-7 transgenic animals where $G\alpha_o$ and synaptic transmission were blocked in defined cells of the egg-laying circuit. As expected from our Ca^{2+} imaging experiments, NLP-7 over-expressing animals accumulated a similar number of eggs as *egl-1(n986dm)* animals lacking HSNs (35.7 ± 1.4 eggs *vs* 33.4 ± 0.9 eggs Figure 7E). Transgenic expression of Pertussis Toxin in HSNs or loss of the EGL-47 receptor weakly suppressed egg accumulation in NLP-7 over-expressing animals (Figure 7E). The suppression of NLP-7 egg-laying defects by Pertussis Toxin expression was specific, as *egl-1(n986dm)* animals developmentally lacking HSNs showed no comparable decrease in egg retention and showed a mild but significant increase (Figure 7E), possibly through co-expression of Pertussis Toxin from the transgene in the NSMs (Tanis *et al.* 2008). Thus, NLP-7 inhibits egg laying, in part, through an inhibitory G protein like $G\alpha_o$ in HSN and the EGL-47 receptor. Because whole-animal, but not HSN-specific, elimination of $G\alpha_o$ function completely suppressed NLP-7-induced egg-laying defects (Figure 7A), these data show that NLP-7 signals to inhibit egg laying through $G\alpha_o$-coupled receptors on cells other than HSN. The cholinergic VC neurons also make extensive synapses onto the vulval muscles, suggesting they may act alongside the HSNs to promote vulval muscle contractility and egg laying (White *et al.* 1986; Waggoner *et al.* 1998). To test whether enhanced VC neurotransmitter release was driving the hyperactive egg-laying behavior of $G\alpha_o$ signaling mutants, we transgenically expressed Tetanus Toxin in the VC neurons using a cell-specific promoter (Bany *et al.* 2003). Loss of VC synaptic

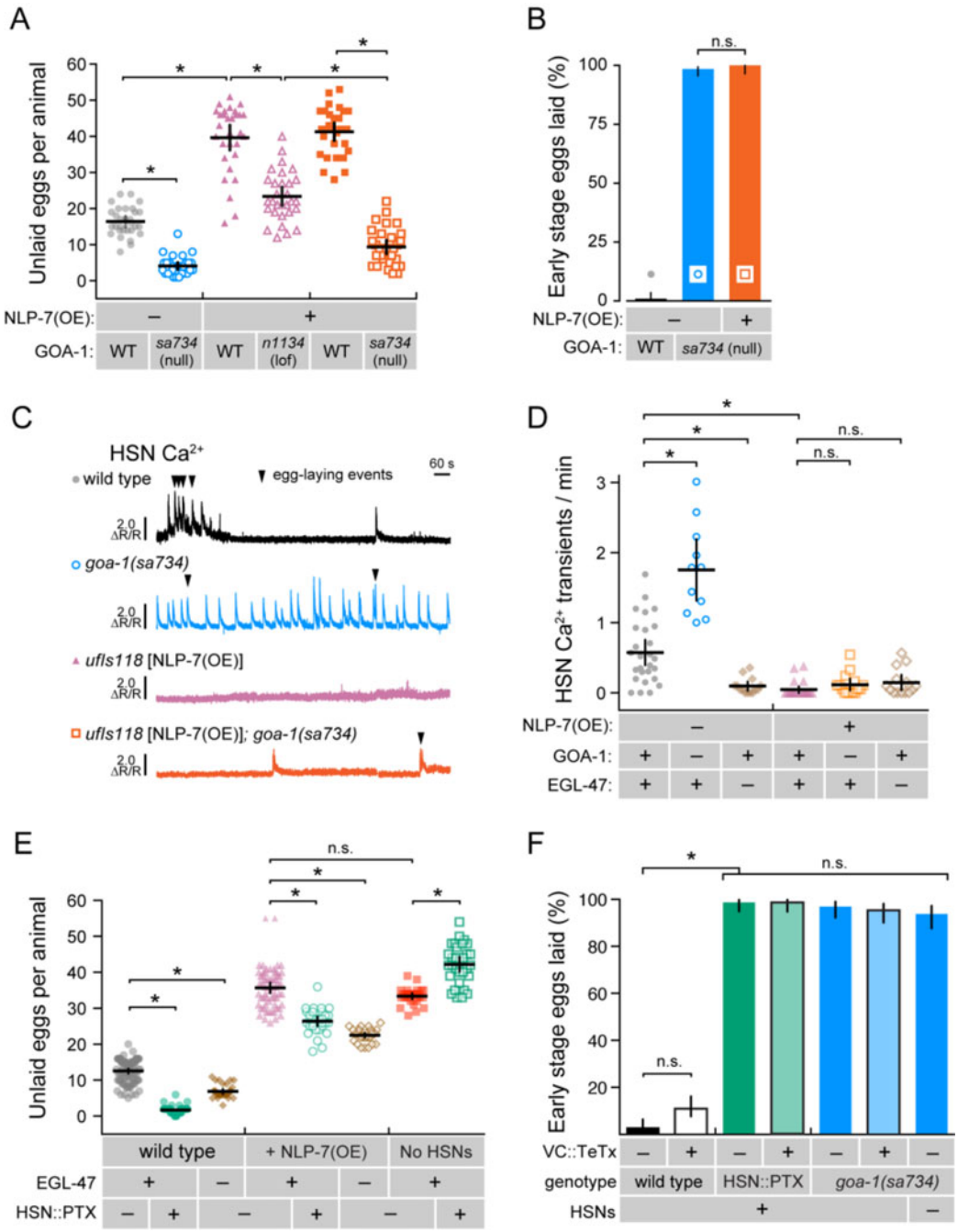

Figure 7 NLP-7 neuropeptides signal through EGL-47 and $G\alpha_o$ to inhibit egg-laying outside of the HSNs. (A) NLP-7 signals through $G\alpha_o$ to inhibit egg-laying behavior. Scatter plots show average number of eggs retained by wild-type (gray circles), *goa-1(sa734)* mutants (blue open circles), NLP-7 over-expressing (OE) transgenics in the wild-type (pink triangles or orange squares), and in NLP-7 over-expressing transgenics in the *goa-1(n1134)* (pink open triangles) and *goa-1(sa734)* null mutant background (orange open squares). Data in orange squares are from animals that also carry the *vsIs183* transgene used for HSN Ca^{2+} imaging. Mean totals below ~10 eggs indicate hyperactive egg laying while totals above ~20 eggs indicate egg-laying defective behavior defects. Error bars indicate 95% confidence intervals for the mean. Asterisks indicate $P < 0.0001$ (one-way ANOVA with Bonferroni correction for multiple comparisons). $N \geq 30$ animals for each strain. (B) Measure of early stage eggs laid by wild-type (black), *goa-1(sa734)* null mutants (blue), and *goa-1(sa734)* null mutants over-expressing NLP-7 neuropeptides (orange). Both *goa-1(sa734)* mutant strains also carry the *vsIs183* transgene used for HSN Ca^{2+} imaging. (C) NLP-7 over-expression silences HSN Ca^{2+} activity. Representative GCaMP5/mCherry ratio traces showing HSN Ca^{2+} activity in wild-type (black), *goa-1(sa734)* null mutants, and NLP-7 overexpressing transgenic animals in the wild-type (pink) and *goa-1(sa734)* null mutant backgrounds (orange). Arrowheads indicate egg-laying events. (D) Scatter plots show HSN Ca^{2+} peaks per minute measurements in wild-type (black), *goa-1(sa734)* null mutants, or *egl-47(ok677)* null mutant animals in the absence or presence of NLP-7 over-expression (OE). Error bars indicate 95% confidence intervals for the mean for $N \geq 10$ animals; n.s. indicates $P > 0.05$ while asterisk indicates $P \leq 0.0001$ (one-way ANOVA with Bonferroni correction for multiple comparisons). (E) NLP-7 inhibition of egg laying is not exclusive to HSN silencing. Scatter plots show the average number of eggs retained by wild-type animals, transgenic animals expressing Pertussis Toxin in HSN, and *egl-47(ok677)* mutant animals in the absence or presence of NLP-7 over-expression (OE) or the absence of HSNs. Error bars indicate 95% confidence intervals for the mean. Asterisks indicate $P < 0.0001$ (one-way ANOVA with Bonferroni correction for multiple comparisons); $N \geq 30$ animals for each strain. (F) Measure of early stage eggs laid by wild-type or transgenic animals expressing Tetanus Toxin the VC neurons (black outlined boxes) in animals expressing Pertussis Toxin in the HSNs (green) or in *goa-1(sa734)* animals missing $G\alpha_o$ (blue). Error bars indicate ± 95% confidence intervals for the mean proportion. Asterisk indicates highlighted significant differences ($P \leq 0.0001$) while n.s. indicates $P > 0.05$ (Fisher Exact Test with Bonferroni correction for multiple comparisons).

transmission had no effect on egg-laying behavior by *goa-1(sa734)* null mutants or animals expressing Pertussis Toxin in HSN (Figure 7F). As previously reported (Mendel *et al.* 1995; Segalat *et al.* 1995), we find that loss of $G\alpha_o$ bypasses the HSNs, as *goa-1(sa734); egl-1(n986dm)* double mutants developmentally missing the HSNs still lay their eggs at early stages of development (Figure 7F). Together, these results show that NLP-7 neuropeptides and $G\alpha_o$ signal to inhibit egg-laying behavior through cellular targets other than the VCs and HSNs.

Discussion

Using a combination of genetic, imaging, physiological, and behavioral approaches, we found that the conserved G protein, $G\alpha_o$, signals to depress activity in the *C. elegans* egg-laying circuit, preventing entry into the active behavior state. Neuropeptides, released in response to aversive external sensory input and feedback of successful egg release, activate inhibitory receptors and $G\alpha_o$ which signal to reduce cell electrical excitability and neurotransmitter release. Without inhibitory $G\alpha_o$ signaling, the presynaptic HSN command neurons remain electrically excited, rendering them resistant to inhibitory sensory input and feedback from the stretch-dependent homeostat. As a result, animals lacking $G\alpha_o$ enter the egg-laying active state twice as frequently as wild-type animals and in environments that would normally be unfavorable for egg laying. Thus, inhibitory $G\alpha_o$ signaling allows for a two-state pattern of circuit activity that can be properly gated by external and internal sensory input.

Our results inform our understanding of how G protein signaling modulates the stretch-dependent homeostat that governs egg-laying behavior. Even in "optimal" environmental conditions including abundant food, egg laying in wild-type animals typically begins ~6 hours after the L4-adult molt upon the accumulation of 5–8 eggs in the uterus (Ravi *et al.* 2018a). Loss of inhibitory $G\alpha_o$ signaling causes precocious egg laying, with eggs being released soon after being deposited into the uterus. Animals lacking $G\alpha_o$ function in HSN show tonic Ca^{2+} transient activity even after chemical sterilization, conditions that normally inhibit HSN and vulval muscle Ca^{2+} activity in wild-type animals. Genetic perturbations that increase inhibitory $G\alpha_o$ signaling delay egg laying until ~18 hours after the molt, like animals lacking HSNs altogether. Egg laying in animals with reduced or eliminated HSN function resumes when the accumulation of eggs activates the circuit via the stretch-dependent homeostat (Collins *et al.* 2016; Ravi *et al.* 2018a). Wild-type animals acutely exposed to aversive sensory conditions show a rapid inhibition of HSN activity and egg laying (Sawin 1996; Zhang *et al.* 2008; Fenk and de Bono 2015), but they continue to make and accumulate eggs in the uterus. Egg laying resumes upon removal of the inhibitory sensory stimulus or a return to food (Sawin 1996; Dong *et al.* 2000). Feedback of egg accumulation and release has long-term consequences on female reproductive physiology. The cGMP-dependent protein kinase G ortholog, EGL-4, regulates the expression of a novel secreted protein in the uterine epithelium whose levels correlate with egg-laying rate (Hao *et al.* 2011). Feedback of egg release regulates *tph-1* gene expression that increases serotonin biosynthesis in the HSNs, alters sensory responses to male pheromone, and germline precursor cell proliferation (Aprison and Ruvinsky 2019a,b). Because the primary function of all adult *C. elegans* behaviors is survival and reproduction, we hypothesize that most or all salient sensory signals ultimately converge to modulate egg-laying circuit activity and animal fecundity.

Our work shows that $G\alpha_o$ also signals in cells other than HSN to inhibit egg-laying circuit activity and behavior. GOA-1 is likely expressed in all electrically excitable cells including all cells in the egg-laying circuit (Mendel *et al.* 1995; Segalat *et al.* 1995; Jose *et al.* 2007). Over-expression of NLP-7 neuropeptides strongly inhibits HSN Ca^{2+} activity and egg-laying behavior. While complete loss of $G\alpha_o$ suppresses egg-laying defects caused by NLP-7 overexpression, HSN Ca^{2+} activity remains largely inhibited. This suggests NLP-7 signals through $G\alpha_o$ to inhibit egg laying in cells other than HSN. Consistent with this result, *goa-1* null mutants remain strongly hyperactive for egg laying even when HSN or VC synaptic transmission is blocked. Where else does $G\alpha_o$ function to inhibit egg laying? While $G\alpha_o$ is expressed in the vulval muscles, transgenic expression of Pertussis Toxin or a GTP-locked form of $G\alpha_o$ causes only modest egg-laying defects. Extensive work has shown that $G\alpha_o$ signals to inhibit release of acetylcholine from motor neurons during locomotion (Miller *et al.* 1999; Nurrish *et al.* 1999). EM reconstruction that revealed the *C. elegans* synaptic wiring diagram shows that the VA7 and VB6 cholinergic motor neurons that drive body wall muscle contraction for locomotion also synapse onto the vm1 vulval muscles (White *et al.* 1986). Recent work employing a new fluorescent reporter of acetylcholine shows rhythmic activity in the vm1 muscles (Borden *et al.* 2020), and this vm1 activity is precisely where we observe weak vulval muscle "twitch" Ca^{2+} transients (Collins *et al.* 2016; Brewer *et al.* 2019). Mutations that increase $G\alpha_s$ and cAMP signaling increase acetylcholine release from motor neurons and promote locomotion (Reynolds *et al.* 2005; Schade *et al.* 2005; Charlie *et al.* 2006a,2006b), possibly explaining why these mutations also increase egg laying. We predict that cholinergic neurons like VA7 and VB6, or their command interneurons, express neuropeptides and neurotransmitter receptors that signal through $G\alpha_o$ to depress acetylcholine release and excitation of the vulval muscles. Identifying where such receptors are expressed and how they signal will help explain how each cell in the circuit functions to drive discrete steps in egg laying (Brewer *et al.* 2019; Fernandez *et al.* 2020).

Our work is consistent with prior work showing $G\alpha_o$ inhibits synaptic transmission via modulation of presynaptic ion channels. Genetic studies in *C. elegans* have identified the IRK inward rectifying K^+ channels, NCA Na^+ leak channels, and CCA-1 T-type voltage-gated Ca^{2+} channels as potential targets of $G\alpha_o$ signaling (Yeh *et al.* 2008; Emtage *et al.* 2012; Zang *et al.* 2017; Topalidou *et al.* 2017b). Inward rectifying GIRK K^+ channels are activated by release of $\beta\gamma$ subunits (Hille 1994). Previous work has shown the IRK-1 K^+ channel is expressed in HSN and is required for inhibition of egg laying by the $G\alpha_o$-coupled EGL-6 neuropeptide receptor (Emtage *et al.* 2012). The egg-laying phenotypes of *irk-1* mutant animals are not as strong as *goa-1* mutants, and our results show that over-expression of $\beta\gamma$ subunits in HSN causes little or no effect on egg laying. These results suggest $G\alpha_o$ signals to inhibit HSN neurotransmitter release via additional mechanism(s). NALCN Na^+ leak channels are also expressed in HSN, and gain-of-function mutations increase HSN Ca^{2+} activity and drive hyperactive egg-laying and locomotion behaviors (Yeh *et al.* 2008). NALCN channels are genetically downstream of both $G\alpha_q$ and $G\alpha_o$ in the regulation of dopamine signaling and locomotion, suggesting that NALCN channels could be direct targets for modulation (Lutas *et al.* 2016; Topalidou *et al.* 2017a). Physiological experiments in mammalian neurons support this model. NALCN currents are activated by neuropeptide signaling through $G\alpha_q$ (Lu *et al.* 2009) and inhibited by dopamine and GABA signaling through $G\alpha_{i/o}$ (Philippart and Khaliq 2018). However, *C. elegans*

knockout mutants in NALCN channel components do not show the strong behavior defects seen in $G\alpha_q$ and $G\alpha_o$ mutants, suggesting other channels act in parallel to NALCN to regulate HSN and circuit excitability. One candidate is TMC channels that drive a background Na^+ leak conductance that promotes HSN and vulval muscle cell electrical excitability (Yue *et al.* 2018). TMC channels may also regulate cell electrical excitability as mechanosensors (Pan *et al.* 2018; Tang *et al.* 2020). Cl^- channels and transporter proteins also regulate HSN activity and egg-laying behavior. CLH-3 is a swelling and hyperpolarization-activated, inwardly rectifying chloride channel that inhibits HSN activity (Branicky *et al.* 2014). Dynamic expression of Cl^- transporter proteins in the HSNs as animals mature into egg-laying adults regulates the Cl^- reversal potential (Tanis *et al.* 2009; Bellemer *et al.* 2011; Han *et al.* 2015). Loss of KCC-2 or ABTS-1 transporters flips the reduced egg laying behavior of *egl-47(dm)* mutants into hyperactive egg laying. Modulation of Cl^- transporter expression or activity by G protein signaling could drive the shifts in cell excitability we observe between the inactive and active egg-laying behavior states.

The modulation of antagonistic cation and anion channels likely determines the Ca^{2+} dependent spiking probability of cells in the egg-laying circuit. HSN expresses L-type, P/Q-type, and T-type voltage-gated Ca^{2+} channels (Mathews *et al.* 2003; Zang *et al.* 2017), and each contributes to a normal serotonin response and egg-laying behavior (Schafer and Kenyon 1995; Lee *et al.* 1997; Kwok *et al.* 2006). The modest but significant changes in HSN resting membrane potential we observe in $G\alpha_o$ signaling mutants are expected to alter the probability of eliciting Ca^{2+} spiking activity. Ca^{2+}-dependent action potentials have been found in *C. elegans* neurons and muscles (Gao and Zhen 2011; Liu *et al.* 2011, 2018) and is regulated by both L-type and T-type Ca^{2+} channels. T-type channels like CCA-1 can contribute to a "window current" where the channel can pass current at depolarized potentials that are insufficient to trigger channel inactivation (Williams *et al.* 1997; Crunelli *et al.* 2005; Zang *et al.* 2017). Activation of these window currents might allow neurons like HSN to shift from spontaneous tonic firing to high-frequency Ca^{2+} bursting. Future work leveraging the powerful molecular tools uniquely available in *C. elegans* and the egg-laying circuit along with direct physiological measurements of membrane potential will allow mechanistic insight into how neuromodulators like serotonin and neuropeptides signal through effectors to shape patterns of circuit activity that underlie distinct behavior states.

Acknowledgments

The authors thank Drs. Jessica Tanis and Michael Koelle for sharing unpublished strains. They thank Yuichi Iino for sharing plasmids. They thank Dr. Addys Bode Hernandez and Michael Scheetz for technical assistance. They also thank Drs. Qiang Liu, James Baker, Julia Dallman, Laura Bianchi, Brock Grill, Peter Larsson, Stephen Roper, along with members of the Collins lab for helpful discussions and feedback on the manuscript.

Funding

This work was funded by grants from the National Institutes of Health (NS086932) and the National Science Foundation (IOS-1844657) to K.M.C. R.J.K. 3rd was supported by a University of Miami Maytag Fellowship. J.M.K. is supported by a grant from the National Institutes of Health (NS032196). Strains used in this study have been provided to the *C. elegans* Genetics Center, which is funded by National Institutes of Health Office of Research Infrastructure Programs (P40 OD010440).

Conflicts of interest

None declared.

Literature cited

Alkema MJ, Hunter-Ensor M, Ringstad N, Horvitz HR. 2005. Tyramine functions independently of octopamine in the *Caenorhabditis elegans* nervous system. Neuron. 46:247–260.

Aprison EZ, Ruvinsky I. 2014. Balanced trade-offs between alternative strategies shape the response of C. elegans reproduction to chronic heat stress. PLoS One. 9:e105513.

Aprison EZ, Ruvinsky I. 2019a. Coordinated behavioral and physiological responses to a social signal are regulated by a shared neuronal circuit. Curr Biol. 29:4108–4115.e4104.

Aprison EZ, Ruvinsky I. 2019b. Dynamic regulation of adult-specific functions of the nervous system by signaling from the reproductive system. Curr Biol. 29:4116–4123.e4113.

Banerjee N, Bhattacharya R, Gorczyca M, Collins KM, Francis MM. 2017. Local neuropeptide signaling modulates serotonergic transmission to shape the temporal organization of *C. elegans* egg-laying behavior. PLoS Genet. 13:e1006697.

Bany IA, Dong MQ, Koelle MR. 2003. Genetic and cellular basis for acetylcholine inhibition of *Caenorhabditis elegans* egg-laying behavior. J Neurosci. 23:8060–8069.

Bastiani CA, Gharib S, Simon MI, Sternberg PW. 2003. *Caenorhabditis elegans* Galphaq regulates egg-laying behavior via a PLCbeta-independent and serotonin-dependent signaling pathway and likely functions both in the nervous system and in muscle. Genetics. 165:1805–1822.

Bellemer A, Hirata T, Romero MF, Koelle MR. 2011. Two types of chloride transporters are required for GABA(A) receptor-mediated inhibition in *C. elegans*. EMBO J. 30:1852–1863.

Borden PM, Zhang P, Shivange AV, Marvin JS, Cichon J, *et al.* 2020. A fast genetically encoded fluorescent sensor for faithful *in vivo* acetylcholine detection in mice, fish, worms and flies. bioRxiv. 2020.2002.2007.939504.

Branicky R, Miyazaki H, Strange K, Schafer WR. 2014. The voltage--gated anion channels encoded by clh-3 regulate egg laying in *C. elegans* by modulating motor neuron excitability. J Neurosci. 34: 764–775.

Brenner S. 1974. The genetics of *Caenorhabditis elegans*. Genetics. 77: 71–94.

Brewer JC, Collins KM, Koelle MR, Olsen A. 2019. Serotonin and neuropeptides are both released by the HSN command neuron to initiate *C. elegans* egg laying. PLoS Genet. 15:e1007896.

Brundage L, Avery L, Katz A, Kim UJ, Mendel JE, *et al.* 1996. Mutations in a *C. elegans* Gqalpha gene disrupt movement, egg laying, and viability. Neuron. 16:999–1009.

Carnell L, Illi J, Hong SW, McIntire SL. 2005. The G-protein-coupled serotonin receptor SER-1 regulates egg laying and male mating behaviors in *Caenorhabditis elegans*. J Neurosci. 25:10671–10681.

C. elegans Deletion Mutant Consortium. 2012. large-scale screening for targeted knockouts in the *Caenorhabditis elegans* genome. G3 (Bethesda). 2:1415–1425.

Charlie NK, Schade MA, Thomure AM, Miller KG. 2006a. Presynaptic UNC-31 (CAPS) is required to activate the G alpha(s) pathway of

the *Caenorhabditis elegans* synaptic signaling network. Genetics. 172:943–961.

Charlie NK, Thomure AM, Schade MA, Miller KG. 2006b. The Dunce cAMP phosphodiesterase PDE-4 negatively regulates G alpha(s)--dependent and G alpha(s)-independent cAMP pools in the *Caenorhabditis elegans* synaptic signaling network. Genetics. 173: 111–130.

Chase DL, Pepper JS, Koelle MR. 2004. Mechanism of extrasynaptic dopamine signaling in *Caenorhabditis elegans*. Nat Neurosci. 7: 1096–1103.

Collins KM, Bode A, Fernandez RW, Tanis JE, Brewer JC, *et al.* 2016. Activity of the *C. elegans* egg-laying behavior circuit is controlled by competing activation and feedback inhibition. eLife. 5: e21126.

Collins KM, Koelle MR. 2013. Postsynaptic ERG potassium channels limit muscle excitability to allow distinct egg-laying behavior states in *Caenorhabditis elegans*. J Neurosci. 33:761–775.

Crunelli V, Toth TI, Cope DW, Blethyn K, Hughes SW. 2005. The 'window' T-type calcium current in brain dynamics of different behavioural states. J Physiol. 562:121–129.

Dempsey CM, Mackenzie SM, Gargus A, Blanco G, Sze JY. 2005. Serotonin (5HT), fluoxetine, imipramine and dopamine target distinct 5HT receptor signaling to modulate *Caenorhabditis elegans* egg-laying behavior. Genetics. 169:1425–1436.

Dong MQ, Chase D, Patikoglou GA, Koelle MR. 2000. Multiple RGS proteins alter neural G protein signaling to allow *C. elegans* to rapidly change behavior when fed. Genes Dev. 14:2003–2014.

Emtage L, Aziz-Zaman S, Padovan-Merhar O, Horvitz HR, Fang-Yen C, *et al.* 2012. IRK-1 potassium channels mediate peptidergic inhibition of *Caenorhabditis elegans* serotonin neurons via a G(o) signaling pathway. J Neurosci. 32:16285–16295.

Esposito G, Schiavi ED, Bergamasco C, Bazzicalupo P. 2007. Efficient and cell specific knock-down of gene function in targeted *C. elegans* neurons. Gene. 395:170–176.

Fenk LA, de Bono M. 2015. Environmental CO2 inhibits *Caenorhabditis elegans* egg-laying by modulating olfactory neurons and evokes widespread changes in neural activity. Proc Natl Acad Sci USA. 112:E3525–E3534.

Fernandez RW, Wei K, Wang EY, Mikalauskaite D, Olson A, *et al.* 2020. Cellular expression and functional roles of all 26 Neurotransmitter GPCRs in the *C. elegans* egg-laying circuit. J Neurosci. 40:7475–7488.

Frokjaer-Jensen C, Davis MW, Hopkins CE, Newman BJ, Thummel JM, *et al.* 2008. Single-copy insertion of transgenes in *Caenorhabditis elegans*. Nat Genet. 40:1375–1383.

Fujiwara M, Hino T, Miyamoto R, Inada H, Mori I, *et al.* 2015. The importance of cGMP signaling in sensory cilia for body size regulation in *Caenorhabditis elegans*. Genetics. 201:1497–1510.

Fujiwara M, Sengupta P, McIntire SL. 2002. Regulation of body size and behavioral state of *C. elegans* by sensory perception and the EGL-4 cGMP-dependent protein kinase. Neuron. 36: 1091–1102.

Gao S, Zhen M. 2011. Action potentials drive body wall muscle contractions in *Caenorhabditis elegans*. Proc Natl Acad Sci USA. 108: 2557–2562.

Garcia J, Collins KM. 2019. The HSN egg-laying command neurons are required for normal defecation frequency in *Caenorhabditis elegans* (II). MicroPubl Biol. doi: 10.17912/10.17912/micropub.biology.000094.

Ghil S, Choi JM, Kim SS, Lee YD, Liao Y, *et al.* 2006. Compartmentalization of protein kinase A signaling by the heterotrimeric G protein Go. Proc Natl Acad Sci USA. 103:19158–19163.

Goulding EH, Schenk AK, Juneja P, MacKay AW, Wade JM, *et al.* 2008. A robust automated system elucidates mouse home cage behavioral structure. Proc Natl Acad Sci USA. 105:20575–20582.

Gurel G, Gustafson MA, Pepper JS, Horvitz HR, Koelle MR. 2012. Receptors and other signaling proteins required for serotonin control of locomotion in *Caenorhabditis elegans*. Genetics. 192: 1359–1371.

Han B, Bellemer A, Koelle MR. 2015. An evolutionarily conserved switch in response to GABA affects development and behavior of the locomotor circuit of *Caenorhabditis elegans*. Genetics. 199: 1159–1172.

Hao Y, Xu N, Box AC, Schaefer L, Kannan K, *et al.* 2011. Nuclear cGMP-dependent kinase regulates gene expression via activity--dependent recruitment of a conserved histone deacetylase complex. PLoS Genet. 7:e1002065.

Harfe BD, Fire A. 1998. Muscle and nerve-specific regulation of a novel NK-2 class homeodomain factor in *Caenorhabditis elegans*. Development. 125:421–429.

Herlitze S, Garcia DE, Mackie K, Hille B, Scheuer T, *et al.* 1996. Modulation of Ca^{2+} channels by G-protein beta gamma subunits. Nature. 380:258–262.

Hille B. 1994. Modulation of ion-channel function by G-protein-coupled receptors. Trends Neurosci. 17:531–536.

Hobson RJ, Hapiak VM, Xiao H, Buehrer KL, Komuniecki PR, *et al.* 2006. SER-7, a *Caenorhabditis elegans* 5-HT7-like receptor, is essential for the 5-HT stimulation of pharyngeal pumping and egg laying. Genetics. 172:159–169.

Horvitz HR, Chalfie M, Trent C, Sulston JE, Evans PD. 1982. Serotonin and octopamine in the nematode *Caenorhabditis elegans*. Science. 216:1012–1014.

Jansen G, Thijssen KL, Werner P, van der Horst M, Hazendonk E, *et al.* 1999. The complete family of genes encoding G proteins of *Caenorhabditis elegans*. Nat Genet. 21:414–419.

Jiang M, Spicher K, Boulay G, Wang Y, Birnbaumer L. 2001. Most central nervous system D2 dopamine receptors are coupled to their effectors by Go. Proc Natl Acad Sci USA. 98:3577–3582.

Jose AM, Bany IA, Chase DL, Koelle MR. 2007. A specific subset of transient receptor potential vanilloid-type channel subunits in *Caenorhabditis elegans* endocrine cells function as mixed heteromers to promote neurotransmitter release. Genetics. 175:93–105.

Jose AM, Koelle MR. 2005. Domains, amino acid residues, and new isoforms of *Caenorhabditis elegans* diacylglycerol kinase 1 (DGK-1) important for terminating diacylglycerol signaling *in vivo*. J Biol Chem. 280:2730–2736.

Kobayashi I, Shibasaki H, Takahashi K, Tohyama K, Kurachi Y, *et al.* 1990. Purification and characterization of five different alpha subunits of guanine-nucleotide-binding proteins in bovine brain membranes. Their physiological properties concerning the activities of adenylate cyclase and atrial muscarinic K^+ channels. Eur J Biochem. 191:499–506.

Koelle MR. 2018. Neurotransmitter signaling through heterotrimeric G proteins: insights from studies in *C. elegans*. WormBook. 1–78.

Koelle MR, Horvitz HR. 1996. EGL-10 regulates G protein signaling in the *C. elegans* nervous system and shares a conserved domain with many mammalian proteins. Cell. 84:115–125.

Kopchock RJ, 3rd, Ravi B, Bode A, Collins KM. 2021. The sex-specific VC Neurons are mechanically activated motor neurons that facilitate Serotonin-induced egg laying in *C. elegans*. J Neurosci. 41: 3635–3650.

Kwok TC, Ricker N, Fraser R, Chan AW, Burns A, *et al.* 2006. A small--molecule screen in *C. elegans* yields a new calcium channel antagonist. Nature. 441:91–95.

Lackner MR, Nurrish SJ, Kaplan JM. 1999. Facilitation of synaptic transmission by EGL-30 Gqalpha and EGL-8 PLCbeta: DAG binding to UNC-13 is required to stimulate acetylcholine release. Neuron. 24:335–346.

Lee RY, Lobel L, Hengartner M, Horvitz HR, Avery L. 1997. Mutations in the alpha1 subunit of an L-type voltage-activated Ca2+ channel cause myotonia in *Caenorhabditis elegans*. EMBO J. 16: 6066–6076.

L'Etoile ND, Coburn CM, Eastham J, Kistler A, Gallegos G, *et al.* 2002. The cyclic GMP-dependent protein kinase EGL-4 regulates olfactory adaptation in *C. elegans*. Neuron. 36:1079–1089.

Li P, Collins KM, Koelle MR, Shen K. 2013. LIN-12/Notch signaling instructs postsynaptic muscle arm development by regulating UNC-40/DCC and MADD-2 in *Caenorhabditis elegans*. eLife. 2: e00378.

Liu P, Ge Q, Chen B, Salkoff L, Kotlikoff MI, *et al.* 2011. Genetic dissection of ion currents underlying all-or-none action potentials in *C. elegans* body-wall muscle cells. J Physiol. 589:101–117.

Liu Q, Kidd PB, Dobosiewicz M, Bargmann CI. 2018. *C. elegans* AWA olfactory neurons fire calcium-mediated all-or-none action potentials. Cell. 175:57–70.e17.

Lou X, Korogod N, Brose N, Schneggenburger R. 2008. Phorbol esters modulate spontaneous and Ca2+-evoked transmitter release via acting on both Munc13 and protein kinase C. J Neurosci. 28: 8257–8267.

Lu B, Su Y, Das S, Wang H, Wang Y, *et al.* 2009. Peptide neurotransmitters activate a cation channel complex of NALCN and UNC-80. Nature. 457:741–744.

Lutas A, Lahmann C, Soumillon M, Yellen G. 2016. The leak channel NALCN controls tonic firing and glycolytic sensitivity of substantia nigra pars reticulata neurons. eLife. 5:e15271

Marder E. 2012. Neuromodulation of neuronal circuits: back to the future. Neuron. 76:1–11.

Mathews EA, Garcia E, Santi CM, Mullen GP, Thacker C, *et al.* 2003. Critical residues of the *Caenorhabditis elegans* unc-2 voltage-gated calcium channel that affect behavioral and physiological properties. J Neurosci. 23:6537–6545.,

Matsubara H. 2002. [Angiotensin II type 2 (AT2) receptor signal and cardiovascular action]. Nihon Yakurigaku Zasshi. 119:95–102.

McMullan R, Hiley E, Morrison P, Nurrish SJ. 2006. Rho is a presynaptic activator of neurotransmitter release at pre-existing synapses in *C. elegans*. Genes Dev. 20:65–76.

McMullan R, Nurrish SJ. 2011. The RHO-1 RhoGTPase modulates fertility and multiple behaviors in adult *C. elegans*. PLoS One. 6: e17265.

McMullen PD, Aprison EZ, Winter PB, Amaral LA, Morimoto RI, *et al.* 2012. Macro-level modeling of the response of *C. elegans* reproduction to chronic heat stress. PLoS Comput Biol. 8:e1002338.

Mendel JE, Korswagen HC, Liu KS, Hajdu-Cronin YM, Simon MI, *et al.* 1995. Participation of the protein Go in multiple aspects of behavior in *C. elegans*. Science. 267:1652–1655.

Miller KG, Emerson MD, Rand JB. 1999. Goalpha and diacylglycerol kinase negatively regulate the Gqalpha pathway in C. elegans. Neuron. 24:323–333.

Mitchell DH, Stiles JW, Santelli J, Sanadi DR. 1979. Synchronous growth and aging of *Caenorhabditis elegans* in the presence of fluorodeoxyuridine. J Gerontol. 34:28–36.

Moresco JJ, Koelle MR. 2004. Activation of EGL-47, a Galpha(o)-coupled receptor, inhibits function of hermaphrodite-specific motor neurons to regulate *Caenorhabditis elegans* egg-laying behavior. J Neurosci. 24:8522–8530.

Mumby SM, Heukeroth RO, Gordon JI, Gilman AG. 1990. G-protein alpha-subunit expression, myristoylation, and membrane association in COS cells. Proc Natl Acad Sci USA. 87:728–732.

Nurrish S, Segalat L, Kaplan JM. 1999. Serotonin inhibition of synaptic transmission: Galpha(0) decreases the abundance of UNC-13 at release sites. Neuron. 24:231–242.

Oikonomou G, Altermatt M, Zhang RW, Coughlin GM, Montz C, *et al.* 2019. The serotonergic raphe promote sleep in Zebrafish and Mice. Neuron. 103:686–701.e688.

Pan B, Akyuz N, Liu XP, Asai Y, Nist-Lund C, *et al.* 2018. TMC1 forms the pore of mechanosensory transduction channels in vertebrate inner ear hair cells. Neuron. 99:736–753.e736.

Patikoglou GA, Koelle MR. 2002. An N-terminal region of *Caenorhabditis elegans* RGS proteins EGL-10 and EAT-16 directs inhibition of G(alpha)o versus G(alpha)q signaling. J Biol Chem. 277: 47004–47013.

Philippart F, Khaliq ZM. 2018. Gi/o protein-coupled receptors in dopamine neurons inhibit the sodium leak channel NALCN. eLife. 7:e40984.

Raizen DM, Cullison KM, Pack AI, Sundaram MV. 2006. A novel gain--of-function mutant of the cyclic GMP-dependent protein kinase egl-4 affects multiple physiological processes in *Caenorhabditis elegans*. Genetics. 173:177–187.

Ravi B, Garcia J, Collins KM. 2018a. Homeostatic feedback modulates the development of two-state patterned activity in a model serotonin motor circuit in *Caenorhabditis elegans*. J Neurosci. 38: 6283–6298.

Ravi B, Nassar LM, Kopchock RJ 3rd, Dhakal P Scheetz, M, *et al.* 2018b. Ratiometric calcium imaging of individual neurons in behaving *Caenorhabditis elegans*. J Vis Exp. 132:56911.

Reuveny E, Slesinger PA, Inglese J, Morales JM, Iniguez-Lluhi JA, *et al.* 1994. Activation of the cloned muscarinic potassium channel by G protein beta gamma subunits. Nature. 370:143–146.

Reynolds NK, Schade MA, Miller KG. 2005. Convergent, RIC-8-dependent Galpha signaling pathways in the *Caenorhabditis elegans* synaptic signaling network. Genetics. 169:651–670.

Ringstad N, Horvitz HR. 2008. FMRFamide neuropeptides and acetylcholine synergistically inhibit egg-laying by *C. elegans*. Nat Neurosci. 11:1168–1176.

Robatzek M, Thomas JH. 2000. Calcium/calmodulin-dependent protein kinase II regulates *Caenorhabditis elegans* locomotion in concert with a G(o)/G(q) signaling network. Genetics. 156:1069–1082.

Sawin ER. 1996. Genetic and Cellular Analysis of Modulated Behaviors in Caenorhabditis elegans. Cambridge, USA: Massachusetts Institute of Technology.

Schade MA, Reynolds NK, Dollins CM, Miller KG. 2005. Mutations that rescue the paralysis of *Caenorhabditis elegans* ric-8 (synembryn) mutants activate the G alpha(s) pathway and define a third major branch of the synaptic signaling network. Genetics. 169: 631–649.

Schafer WF. 2006. Genetics of egg-laying in worms. Annu Rev Genet. 40:487–509.

Schafer WR, Kenyon CJ. 1995. A calcium-channel homologue required for adaptation to dopamine and serotonin in *Caenorhabditis elegans*. Nature. 375:73–78.

Segalat L, Elkes DA, Kaplan JM. 1995. Modulation of serotonin-controlled behaviors by Go in *Caenorhabditis elegans*. Science. 267: 1648–1651.

Shen K, Fetter RD, Bargmann CI. 2004. Synaptic specificity is generated by the synaptic guidepost protein SYG-2 and its receptor, SYG-1. Cell. 116:869–881.

Shyn SI, Kerr R, Schafer WR. 2003. Serotonin and Go modulate functional states of neurons and muscles controlling *C. elegans* egg-laying behavior. Curr Biol. 13:1910–1915.

Taghert PH, Nitabach MN. 2012. Peptide neuromodulation in invertebrate model systems. Neuron. 76:82–97.

Tang YQ, Lee SA, Rahman M, Vanapalli SA, Lu H, *et al.* 2020. Ankyrin is an intracellular tether for TMC mechanotransduction channels. Neuron. 107:759–761.

Tanis JE, Bellemer A, Moresco JJ, Forbush B, Koelle MR. 2009. The potassium chloride cotransporter KCC-2 coordinates development of inhibitory neurotransmission and synapse structure in *Caenorhabditis elegans*. J Neurosci. 29:9943–9954.

Tanis JE, Moresco JJ, Lindquist RA, Koelle MR. 2008. Regulation of serotonin biosynthesis by the G proteins Galphao and Galphaq controls serotonin signaling in *Caenorhabditis elegans*. Genetics. 178: 157–169.

Topalidou I, Chen PA, Cooper K, Watanabe S, Jorgensen EM, *et al.* 2017a. The NCA-1 and NCA-2 Ion channels function downstream of Gq and Rho to regulate locomotion in *Caenorhabditis elegans*. Genetics. 206:265–282.

Topalidou I, Cooper K, Pereira L, Ailion M. 2017b. Dopamine negatively modulates the NCA ion channels in *C. elegans*. PLoS Genet. 13:e1007032.

Trent C. 1982. Genetic and Behavioral Studies of the Egg-Laying System of Caenorhabditis elegans. Cambridge, USA: Massachusetts Institute of Technology.

Trent C, Tsuing N, Horvitz HR. 1983. Egg-laying defective mutants of the nematode *Caenorhabditis elegans*. Genetics. 104:619–647.

Waggoner LE, Hardaker LA, Golik S, Schafer WR. 2000. Effect of a neuropeptide gene on behavioral states in *Caenorhabditis elegans* egg-laying. Genetics. 154:1181–1192.

Waggoner LE, Zhou GT, Schafer RW, Schafer WR. 1998. Control of alternative behavioral states by serotonin in *Caenorhabditis elegans*. Neuron. 21:203–214.

White JG, Southgate E, Thomson JN, Brenner S. 1986. The structure of the nervous system of the nematode *Caenorhabditis elegans*. Philos Trans R Soc Lond B Biol Sci. 314:1–340.

Wierda KD, Toonen RF, de Wit H, Brussaard AB, Verhage M. 2007. Interdependence of PKC-dependent and PKC-independent pathways for presynaptic plasticity. Neuron. 54:275–290.

Williams SL, Lutz S, Charlie NK, Vettel C, Ailion M, *et al.* 2007. Trio's Rho-specific GEF domain is the missing Galpha q effector in *C. elegans*. Genes Dev. 21:2731–2746.,

Williams SR, Toth TI, Turner JP, Hughes SW, Crunelli V. 1997. The 'window' component of the low threshold Ca^{2+} current produces input signal amplification and bistability in cat and rat thalamocortical neurones. J Physiol. 505:689–705.

Yamada K, Hirotsu T, Matsuki M, Kunitomo H, Iino Y. 2009. GPC-1, a G protein gamma-subunit, regulates olfactory adaptation in *Caenorhabditis elegans*. Genetics. 181:1347–1357.

Yawo H. 1999. Protein kinase C potentiates transmitter release from the chick ciliary presynaptic terminal by increasing the exocytotic fusion probability. J Physiol. 515:169–180.

Yeh E, Ng S, Zhang M, Bouhours M, Wang Y, *et al.* 2008. A putative cation channel, NCA-1, and a novel protein, UNC-80, transmit neuronal activity in *C. elegans*. PLoS Biol. 6:e55.

Yue X, Zhao J, Li X, Fan Y, Duan D, *et al.* 2018. TMC proteins modulate egg laying and membrane excitability through a background leak conductance in *C. elegans*. Neuron. 97:571–585.e575.

Zang KE, Ho E, Ringstad N. 2017. Inhibitory peptidergic modulation of *C. elegans* serotonin neurons is gated by T-type calcium channels. eLife. 6:e22771.

Zhang J, Pratt RE. 1996. The AT2 receptor selectively associates with Gialpha2 and Gialpha3 in the rat fetus. J Biol Chem. 271: 15026–15033.

Zhang M, Chung SH, Fang-Yen C, Craig C, Kerr RA, *et al.* 2008. A self-regulating feed-forward circuit controlling *C. elegans* egg-laying behavior. Curr Biol. 18:1445–1455.

Zou W, Fu J, Zhang H, Du K, Huang W, *et al.* 2018. Decoding the intensity of sensory input by two glutamate receptors in one *C. elegans* interneuron. Nat Commun. 9:4311.

Communicating editor: H. Bülow